Angular momentum gain by electrons under the action of intense structured light

E. Dmitriev and Ph. Korneev[*]

P.N. Lebedev Physical Institute of RAS, 53 Leninskii Prospekt, 119991 Moscow, Russian Federation

The problem of the interaction of light waves with charged particles becomes increasingly complex starting with the case of plane waves, where the analytical solution is well known, to more natural, though more complicated situations which include focused or structured laser beams. Internal structure may introduce a new degree of freedom and qualitatively change the dynamics of interacting particles. For certain conditions, namely, for the dilute plasma, a description of single-particle dynamics in the focused structured laser beams is the first step and may serve as a good approximation to understand the global plasma response. Moreover, the general problem of integrability in complex systems starts from a consideration of the integrals of motion for a single particle. The primary goal of this work is an understanding of the physics of the orbital angular momentum (OAM) absorption by a single particle in a focused structured light. A theoretical model of the process, including solutions of Maxwell equations with the required accuracy and a high-order perturbative approach to electron motion in external electromagnetic fields, is developed and its predictions are examined with numerical simulations for several exemplary electromagnetic field configurations. In particular, it was found that for the particles which are initially distributed with the azimuthal symmetry around the beam propagation direction, the transferred OAM has a smallness of the fourth order of the applied field amplitude and requires an accurate consideration of the temporal laser pulse envelope.

I. INTRODUCTION

Electromagnetic interaction between structured light and charged particles in vacuum may result in particle acceleration, i.e., momentum and energy transfer, which, under certain conditions, appears to be irreversible. For that, the light wave should at least be sufficiently different from a slow-varying plane wave; see, e.g., [1]. In this general context, similar questions may be posed concerning the transfer of the light orbital angular momentum (OAM): how effective is its occurrence when a structured light wave interacts in vacuum with a single charged particle, and how effective is it, on average, for a particle ensemble with a given distribution?

These questions were recently addressed within different frameworks. In [2–4], the OAM transfer is considered numerically for different model configurations of laser beams interacting with individual charged particles in free space. Paraxial and slowly varying envelope approximations were used to prescribe the electromagnetic fields, and specific cases of linear, circular, and radial polarizations with and without spatiotemporal coupling were considered. Transferred energy, momentum, and angular momentum dependence on the duration, amplitude, and other parameters were studied in certain cases. In Ref. [5], numerical simulation of the action of the OAM laser beam on free electrons is presented for the case of a superposition of linearly polarized Laguerre-Gaussian and Gaussian modes; the OAM transfer is estimated based on the

results of the perturbation theory. The importance of the accurate use of the paraxial and slowly varying temporal envelope approximations in numerical simulations is discussed in [6] based on consideration of a conserved integral of motion for the special case, when the circular polarization and orbital momentum in the beam have opposite directions so that there is no dependence on the angle in the phase. The necessity of corrections to the lowest-order approximations both in numerical simulations and analytics is demonstrated.

More complicated, though less detailed studies of the OAM beam interaction with plasmas were mainly performed with the use of large-scale three-dimensional (3D) Particle-in-Cell (PIC) simulations. In Refs. [7,8], the generation of magnetic fields in dilute plasma was observed and explained as a result of an OAM transfer from the laser beam to electrons. There, radial and linear polarizations were considered, showing effective OAM transfer for moderate relativistic intensities. Analysis with the use of simplified electromagnetic fields showed the importance of the longitudinal particle motion for the OAM transfer. The magnetic field was also observed in plasma in Ref. [9] via OAM transfer from two beating Laguerre-Gaussian beams to charged particles. There, a fluid model of the interaction was developed to describe the formation of azimuthal currents in the plasma.

In the case of dissipative processes, the magnetic field generation, originating from angular momentum absorption of a circularly polarized laser beam, is demonstrated theoretically in [10]. Circularly polarized beams were replaced by linearly polarized beams with OAM in Ref. [11]. For intense relativistic beams with different polarizations, including linearly and circularly polarized Laguerre-Gaussian modes, Ref. [12]

[*]Contact author: ph.korneev@gmail.com; korneev@theor.mephi.ru

studies magnetic field generation and dissipative effects in plasma.

Although there is a common conclusion that the OAM transfer from a structured light wave to electrons may be both possible and effective, still, it is not clear if this is always a single-particle effect or if certain nonlinearities originated from collective or dissipative effects are required. It was observed in several studies [3,7], that the individual electrons are absorbing positive or negative light OAM depending on their spatial position, even for a definite OAM sign in the incident wave, but the net gain appears to be much less. The detailed consideration for the analytically attainable special case, predicting no net OAM gain after interaction [6], supported the conclusion that the total OAM transfer is a very delicate process.

In this work, a general problem of OAM transfer from a structured light wave to an ensemble of charged particles is considered for moderate intensities of the incident light. It may be a rarefied plasma, consisting of ions and electrons, which are interacting with an incident light much stronger than with each other, which requires $\omega_p \ll \omega_0$, where $\omega_p = \sqrt{\frac{4\pi n_e e^2}{m_e}}$ is the plasma frequency, n_e is the electron density, e and m_e are the electron charge and mass, respectively, and ω_0 is the characteristic light frequency, e.g., the main carrier frequency of the laser wave. The particles are considered initially cold with the temperature $T \ll (eE_0)^2/(m_e\omega_0^2)$, where E_0 is the electric field amplitude. This condition means that the work performed by the laser wave during one period is small compared to the thermal energy of the electrons and allows one to treat electrons as being at rest before the interaction. Electrons, being the lighter particles, are primarily affected by the light, so the OAM transfer would be analyzed having in mind, namely, the wave-electron interaction, but of course all the results are valid for any charged particles.

First, a perturbation theory on the field strength for arbitrary fields is developed up to the fourth order, to obtain a nonzero net absorbed OAM in the case of homogeneous distribution of the particles. Then, assuming a focused laser beam, an approximate description of the structured wave within the paraxial and the slow temporal dependence approximations is represented. Using this description, several certain configurations are considered in detail, including a comparison with numerical single-particle calculations. Finally, a general discussion and conclusions are presented.

II. ANALYTICAL MODEL

Electron motion in arbitrary electromagnetic fields $\mathbf{E}$ and $\mathbf{H}$ is described by the equation

$$\frac{d\mathbf{p}}{dt} = -e\left(\mathbf{E} + \frac{\mathbf{v}}{c} \times \mathbf{H}\right), \tag{1}$$

with initial conditions

$$\mathbf{r}(t \to -\infty) = \mathbf{r}_0,$$
$$\mathbf{v}(t \to -\infty) = 0, \tag{2}$$

where $\mathbf{p} = m_e\gamma\mathbf{v}$ is the electron momentum, $\gamma = 1/\sqrt{1 - \frac{v^2}{c^2}}$ is the Lorentz factor, $\mathbf{r}_0$ is the electron initial position, c is the
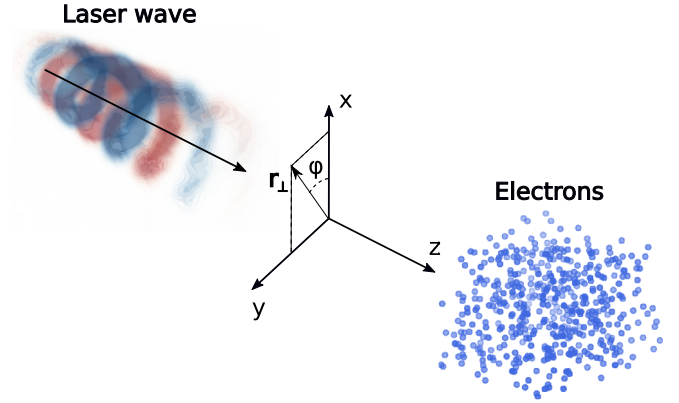

FIG. 1. The interaction scheme and the coordinate system. The z axis coincides with the laser propagation axis and particles are distributed isotropically in the transverse plane xy for every value of z.

light velocity, and $\mathbf{E} = \mathbf{E}(\mathbf{r}, t)$ and $\mathbf{H} = \mathbf{H}(\mathbf{r}, t)$ are the laser electric and magnetic fields respectively, satisfying Maxwell equations in vacuum,

$$\nabla \times \mathbf{E} = -\frac{1}{c}\frac{\partial \mathbf{H}}{\partial t}, \quad \nabla \times \mathbf{H} = \frac{1}{c}\frac{\partial \mathbf{E}}{\partial t}, \tag{3}$$

$$\nabla \cdot \mathbf{H} = 0, \quad \nabla \cdot \mathbf{E} = 0. \tag{4}$$

The schematic setup of the interaction is presented in Fig. 1. In the following, a perturbation theory of angular momentum transfer from electromagnetic wave to charged particles is developed.

A. Particle motion in electromagnetic wave

Formally consider a low-intensity regime $a_0 \ll 1$, where $a_0 = eE_0/(m_e\omega_0 c)$ is the dimensionless amplitude of the field, with E_0 the amplitude of the electric field. The electromagnetic wave is assumed to be finite, $\mathbf{E}(\mathbf{r}, t \to \pm\infty) = \mathbf{H}(\mathbf{r}, t \to \pm\infty) = 0$. In frames of the perturbation theory on a_0, the coordinates and velocities of the particle may be expressed in the form

$$\mathbf{r} = \mathbf{r}^{(0)} + \mathbf{r}^{(1)} + \mathbf{r}^{(2)} + \cdots,$$
$$\mathbf{v} = \mathbf{v}^{(0)} + \mathbf{v}^{(1)} + \mathbf{v}^{(2)} + \cdots, \tag{5}$$

where $\mathbf{r}^{(0)}$ and $\mathbf{v}^{(0)}$ are the unperturbed coordinate and velocity, $\mathbf{r}^{(n)} \sim a_0^n$ and $\mathbf{v}^{(n)} \sim a_0^n$. According to the initial conditions (2), $\mathbf{r}^{(0)} = \mathbf{r}_0$ and $\mathbf{v}^{(0)} = 0$.

In the first order,

$$\frac{d\mathbf{p}^{(1)}}{dt} = -\frac{m_e c\omega_0}{E_0}a_0\mathbf{E}(\mathbf{r}_0, t). \tag{6}$$

The solution of the equation of the first order is

$$\mathbf{p}^{(1)} = m_e\mathbf{v}^{(1)} = -\frac{m_e c\omega_0}{E_0}a_0\int_{-\infty}^{t} dt'\mathbf{E}(\mathbf{r}_0, t'),$$

$$\mathbf{r}^{(1)} = -\frac{c\omega_0}{E_0}a_0\int_{-\infty}^{t} dt'\int_{-\infty}^{t'} dt''\mathbf{E}(\mathbf{r}_0, t''). \tag{7}$$

The gained momentum of a particle in the first order is

$$\mathbf{p}^{(1)}(t_\infty) = -\frac{m_e c \omega_0}{E_0} a_0 \mathbf{E}(\omega = 0, \mathbf{r}_0) = 0, \qquad (8)$$

where the notation $t_\infty \equiv t \to \infty$ is used and $\mathbf{E}(\omega, \mathbf{r})$ is the Fourier component of the electric field. It is assumed that the electromagnetic pulse has no constant part and hence a particle does not gain momentum in the first order. Assuming the same for double integration over time, we obtain

$$\mathbf{r}^{(1)}(t_\infty) = 0. \qquad (9)$$

The validity of this assumption is discussed in more detail in Sec. IV.

According to (8), angular momentum in the first order on a_0 is not gained by a particle,

$$\mathbf{L}^{(1)} = \mathbf{r}_0 \times \mathbf{p}^{(1)} \underset{t_\infty}{\to} 0. \qquad (10)$$

In the second-order perturbation theory,

$$\frac{d\mathbf{p}^{(2)}}{dt} = m_e \frac{d\mathbf{v}^{(2)}}{dt}$$
$$= -\frac{m_e c \omega_0}{E_0} a_0 \left[(\mathbf{r}^{(1)} \cdot \boldsymbol{\nabla}_0) \mathbf{E}(\mathbf{r}_0, t) + \frac{\mathbf{v}^{(1)}}{c} \times \mathbf{H}(\mathbf{r}_0, t) \right], \qquad (11)$$

where $\boldsymbol{\nabla}_0 = \mathbf{e}_x \frac{\partial}{\partial x_0} + \mathbf{e}_y \frac{\partial}{\partial y_0} + \mathbf{e}_z \frac{\partial}{\partial z_0}$ is the del operator, taken with respect to the initial position of the particle $\mathbf{r}_0$.

To obtain general expressions for arbitrary electromagnetic fields, consistent with the Maxwell equations, the perturbation theory uses the relations between the electric and magnetic field components. For $\boldsymbol{\nabla}_0 \times \mathbf{v}^{(1)}$, taking into account that $\boldsymbol{\nabla} \times \mathbf{E} = -\frac{1}{c} \frac{\partial \mathbf{H}}{\partial t}$, one obtains

$$\boldsymbol{\nabla}_0 \times \mathbf{v}^{(1)} = -\frac{c \omega_0}{E_0} a_0 \int_{-\infty}^{t} \boldsymbol{\nabla}_0 \times \mathbf{E}(\mathbf{r}_0, t') dt'$$
$$= \frac{\omega_0}{E_0} a_0 \int_{-\infty}^{t} \frac{\partial \mathbf{H}(\mathbf{r}_0, t')}{\partial t'} dt' = \frac{\omega_0}{E_0} a_0 \mathbf{H}(\mathbf{r}_0, t), \qquad (12)$$

and substituting $\mathbf{H} = \frac{E_0}{\omega_0 a_0} \boldsymbol{\nabla}_0 \times \mathbf{v}^{(1)}$ into (11),

$$\frac{d}{dt} \left[\mathbf{p}^{(2)} - m_e (\mathbf{r}^{(1)} \cdot \boldsymbol{\nabla}_0) \mathbf{v}^{(1)} \right] = -\frac{m_e}{2} \boldsymbol{\nabla}_0 (\mathbf{v}^{(1)})^2. \qquad (13)$$

The gained momentum in the second order after interaction

then reads

$$\mathbf{p}^{(2)}(t_\infty) = -\frac{m_e}{2} \boldsymbol{\nabla}_0 \int_{-\infty}^{\infty} (\mathbf{v}^{(1)})^2 dt, \qquad (14)$$

where it is assumed that $\frac{\partial}{\partial x_i} \mathbf{v}^{(1)}(t_\infty) \to 0$. The particle displacement in the second-order perturbation theory then reads

$$\mathbf{r}^{(2)} = \int_{-\infty}^{t} dt (\mathbf{r}^{(1)} \cdot \boldsymbol{\nabla}_0) \mathbf{v}^{(1)}$$
$$- \frac{1}{2} \int_{-\infty}^{t} dt' \int_{-\infty}^{t'} dt'' \boldsymbol{\nabla}_0 (\mathbf{v}^{(1)})^2. \qquad (15)$$

The second-order absorbed angular momentum is

$$\mathbf{L}^{(2)} = \mathbf{r}_0 \times \mathbf{p}^{(2)} + \mathbf{r}^{(1)} \times \mathbf{p}^{(1)}. \qquad (16)$$

We introduce cylindrical coordinates $(r_\perp, \varphi, z)$, with $r_\perp$ and φ being the transverse distance and the azimuthal angle respectively, i.e., $x = r_\perp \cos\varphi$, $y = r_\perp \cos\varphi$. Axis z is chosen in such a way that it coincides with the axis of propagation of the electromagnetic wave; see Fig. 1 and Sec. II B for further details related to the fields. The longitudinal component of the angular momentum after interaction reads

$$L_z^{(2)}(t_\infty) = r_0 p_\varphi^{(2)}(t_\infty) = -\frac{m_e}{2} \frac{\partial}{\partial \varphi_0} \int_{-\infty}^{\infty} (\mathbf{v}^{(1)})^2 dt, \qquad (17)$$

where $\mathbf{r}_0 \equiv (r_{\perp 0}, \varphi_0, z_0) \equiv (r_0, \varphi_0, z_0)$. After averaging over the azimuthal angle,

$$\langle L_z^{(2)}(t_\infty) \rangle_{\varphi_0} \equiv \frac{\int_0^{2\pi} \rho(r_0, z_0) L_z^{(2)}(t_\infty) d\varphi_0}{\int_0^{2\pi} \rho(r_0, z_0) d\varphi_0}$$
$$= \frac{1}{2\pi} \int_0^{2\pi} L_z^{(2)}(t_\infty) d\varphi_0 = 0, \qquad (18)$$

where the distribution function of the initial coordinates of the particles $\rho(r_0, z_0)$ is considered to be symmetric about the laser propagation axis, i.e., it does not depend on the initial angle of the particle φ_0. For instance, the distribution function for an isotropic plasma cylinder is $\rho(r_0, z_0) = 1/(\pi R^2 h)$ for r_0, z_0 that are inside the cylinder, and 0 otherwise, where R is the radius and h is the height of the cylinder, respectively.

As it follows from (18), for the plasma, which is transversely isotropic to the wave propagation direction, there is no net angular momentum gain up to the second order of the perturbation theory on a_0; to describe the angular momentum transfer, higher orders of perturbation theory are required.

The third-order perturbation theory gives, for the momentum,

$$\frac{d\mathbf{p}^{(3)}}{dt} = -\frac{m_e c \omega_0}{E_0} a_0 \left[(\mathbf{r}^{(2)} \cdot \boldsymbol{\nabla}_0) \mathbf{E}(\mathbf{r}_0, t) + \frac{1}{2} r_\alpha^{(1)} r_\beta^{(1)} \frac{\partial^2 \mathbf{E}(\mathbf{r}_0, t)}{\partial r_{0\alpha} r_{0\beta}} + \frac{\mathbf{v}^{(2)}}{c} \times \mathbf{H}(\mathbf{r}_0, t) + \frac{\mathbf{v}^{(1)}}{c} \times (\mathbf{r}^{(1)} \cdot \boldsymbol{\nabla}_0) \mathbf{H}(\mathbf{r}_0, t) \right] \qquad (19)$$

or, after some algebra,

$$\frac{d}{dt} \left\{ \mathbf{p}^{(3)} - m_e (\mathbf{r}^{(2)} \cdot \boldsymbol{\nabla}_0) \mathbf{v}^{(1)} - \frac{m_e}{2} r_\alpha^{(1)} r_\beta^{(1)} \frac{\partial^2 \mathbf{v}^{(1)}}{\partial r_{0\alpha} \partial r_{0\beta}} + m_e v_\alpha^{(2)} \boldsymbol{\nabla}_0 r_\alpha^{(1)} - m_e [(\mathbf{r}^{(1)} \cdot \boldsymbol{\nabla}_0) v_\alpha^{(1)}] \boldsymbol{\nabla}_0 r_\alpha^{(1)} \right\} = -\frac{m_e}{2} \boldsymbol{\nabla}_0 \{ \boldsymbol{\nabla}_0 \cdot [\mathbf{r}^{(1)} (\mathbf{v}^{(1)})^2] \}. \qquad (20)$$

Then a particle after interaction gains the momentum

$$\mathbf{p}^{(3)}(t_\infty) = -\frac{m_e}{2} \boldsymbol{\nabla}_0 \left[\boldsymbol{\nabla}_0 \cdot \int_{-\infty}^{\infty} \mathbf{r}^{(1)} (\mathbf{v}^{(1)})^2 dt \right], \qquad (21)$$

where it is additionally assumed that $\frac{\partial}{\partial x_{0i}}\mathbf{r}^{(1)}(t_\infty) \to 0$. The absorbed angular momentum in the third order of the perturbation theory may be represented as

$$\mathbf{L}^{(3)} = \mathbf{r}_0 \times \mathbf{p}^{(3)} + \mathbf{r}^{(1)} \times \mathbf{p}^{(2)} + \mathbf{r}^{(2)} \times \mathbf{p}^{(1)}. \tag{22}$$

This value may appear to be nonzero for certain particles, but for isotropic plasma it again vanishes after averaging,

$$L_z^{(3)}(t \to \infty) = -\frac{m_e}{2}\frac{\partial}{\partial \varphi_0}\left[\nabla_0 \cdot \int_{-\infty}^{\infty}\mathbf{r}^{(1)}(\mathbf{v}^{(1)})^2 dt\right] \xrightarrow[\langle \dots \rangle_{\varphi_0}]{} 0. \tag{23}$$

In the fourth order of the perturbation theory, the particle momentum reads

$$\frac{d\mathbf{p}^{(4)}}{dt} = \frac{m_e c \omega_0}{E_0}a_0\left\{(\mathbf{r}^{(3)} \cdot \nabla_0)\mathbf{E}(\mathbf{r}_0, t) + r_\alpha^{(1)}r_\beta^{(2)}\frac{\partial^2 \mathbf{E}(\mathbf{r}_0, t)}{\partial r_{0\alpha}\partial r_{0\beta}} + \frac{1}{6}r_\alpha^{(1)}r_\beta^{(1)}r_\gamma^{(1)}\frac{\partial^3 \mathbf{E}(\mathbf{r}_0, t)}{\partial r_{0\alpha}\partial r_{0\beta}\partial r_{0\gamma}} + \frac{\mathbf{v}^{(3)}}{c} \times \mathbf{H}(\mathbf{r}_0, t)\right.$$
$$\left. + \frac{\mathbf{v}^{(2)}}{c} \times (\mathbf{r}^{(1)} \cdot \nabla_0)\mathbf{H}(\mathbf{r}_0, t) + \frac{\mathbf{v}^{(1)}}{c} \times \left[(\mathbf{r}^{(2)} \cdot \nabla_0)\mathbf{H}(\mathbf{r}_0, t) + \frac{1}{2}r_\alpha^{(1)}r_\beta^{(1)}\frac{\partial^2 \mathbf{H}(\mathbf{r}_0, t)}{\partial r_{0\alpha}\partial r_{0\beta}}\right]\right\}. \tag{24}$$

This expression may be represented as

$$\frac{d}{dt}\left\{\mathbf{p}^{(4)} - m_e(\mathbf{r}^{(3)} \cdot \nabla_0)\mathbf{v}^{(1)} - m_e r_\alpha^{(1)}r_\beta^{(2)}\frac{\partial^2 \mathbf{v}^{(1)}}{\partial r_{0\alpha}\partial r_{0\beta}} - \frac{m_e}{6}r_\alpha^{(1)}r_\beta^{(1)}r_\gamma^{(1)}\frac{\partial^3 \mathbf{v}^{(1)}}{\partial r_{0\alpha}\partial r_{0\beta}\partial r_{0\gamma}}\right.$$
$$+ m_e v_\alpha^{(3)}\nabla_0 r_\alpha^{(1)} - m_e\left[(\mathbf{r}^{(2)} \cdot \nabla_0)v_\alpha^{(1)}\right]\nabla_0 r_\alpha^{(1)} - \frac{m_e}{2}r_\alpha^{(1)}r_\beta^{(1)}\frac{\partial^2 v_\gamma^{(1)}}{\partial r_{0\alpha}\partial r_{0\beta}}\nabla_0 r_\gamma^{(1)}$$
$$\left. + \frac{m_e}{2c^2}(\mathbf{v}^{(1)})^2 v_\alpha^{(1)}\nabla_0 r_\alpha^{(1)} + m_e(\mathbf{r}^{(2)}\nabla_0)\left[(\mathbf{r}^{(1)} \cdot \nabla_0)\mathbf{v}^{(1)}\right]\right\}$$
$$= \frac{m_e}{8c^2}\nabla_0(\mathbf{v}^{(1)})^4 - \frac{m_e}{2}\nabla_0\left(r_\alpha^{(1)}r_\beta^{(1)}v_\gamma^{(1)}\frac{\partial^2 v_\gamma^{(1)}}{\partial r_{0\alpha}\partial r_{0\beta}}\right) - \frac{m_e}{2}\nabla_0(\mathbf{v}^{(2)})^2 + m_e\frac{d}{dt}\left[(\mathbf{r}^{(2)} \cdot \nabla_0)\mathbf{v}^{(2)}\right], \tag{25}$$

where it is taken into account that $\nabla \cdot \mathbf{r}^{(1)} = 0$ since $\nabla \cdot \mathbf{E}(\mathbf{r}_0, t) = 0$. The angular momentum, gained by a single particle in the fourth order reads

$$\mathbf{L}^{(4)} = \mathbf{r}_0 \times \mathbf{p}^{(4)} + \mathbf{r}^{(1)} \times \mathbf{p}^{(3)} + \mathbf{r}^{(2)} \times \mathbf{p}^{(2)} + \mathbf{r}^{(3)} \times \mathbf{p}^{(1)}. \tag{26}$$

After averaging its longitudinal component over the azimuthal angle, at $t \to \infty$ it becomes

$$\left\langle L_z^{(4)}(t_\infty)\right\rangle_{\varphi_0} = m_e\langle[\mathbf{r}_0 \times (\mathbf{r}^{(2)} \cdot \nabla_0)\mathbf{v}^{(2)}]_z + (\mathbf{r}^{(2)} \times \mathbf{p}^{(2)})_z\rangle_{\varphi_0}\big|_{t_\infty} = \left\langle[\mathbf{r}^{(2)}(t_\infty) \cdot \nabla_0]L_z^{(2)}(t_\infty)\right\rangle_{\varphi_0}, \tag{27}$$

which is not zero in general. For the subsequent analysis, here we also present the expression for the particle energy up to the fourth order of the perturbation theory,

$$m_e c^2 \gamma = \frac{m_e c^2}{\sqrt{1 - \mathbf{v}^2/c^2}} \approx m_e c^2 + \frac{m_e}{2}\left[(\mathbf{v}^{(1)})^2 + 2(\mathbf{v}^{(1)} \cdot \mathbf{v}^{(2)}) + 2(\mathbf{v}^{(1)} \cdot \mathbf{v}^{(3)}) + (\mathbf{v}^{(2)})^2\right] + \frac{3m_e}{8c^2}(\mathbf{v}^{(1)})^4. \tag{28}$$

After the interaction ends, the first nonvanishing contribution to the total kinetic energy gain is also of the fourth order,

$$m_e c^2(\gamma - 1)|_{t_\infty} \equiv \varepsilon|_{t_\infty} \approx \varepsilon^{(4)}(t_\infty) = \frac{m_e}{2}[\mathbf{v}^{(2)}(t_\infty)]^2. \tag{29}$$

We gather the obtained expressions for the momentum, the angular momentum, the average angular momentum, and the energy gained by particles in the main nonvanishing order of the perturbation theory on a_0:

$$\mathbf{p}^{(2)}(t_\infty) = -\frac{m_e}{2}\nabla_0\int_{-\infty}^{\infty}[\mathbf{v}^{(1)}(\mathbf{r}_0, t)]^2 dt, \quad L_z^{(2)}(t_\infty) = -\frac{m_e}{2}\frac{\partial}{\partial \varphi_0}\int_{-\infty}^{\infty}[\mathbf{v}^{(1)}(\mathbf{r}_0, t)]^2 dt,$$

$$\left\langle L_z^{(4)}(t_\infty)\right\rangle_{\varphi_0} = \left\langle[\mathbf{r}^{(2)}(\mathbf{r}_0, t_\infty) \cdot \nabla_0]L_z^{(2)}(\mathbf{r}_0, t_\infty)\right\rangle_{\varphi_0}, \quad \varepsilon^{(4)}(t_\infty) = \frac{m_e}{2}[\mathbf{v}^{(2)}(\mathbf{r}_0, t_\infty)]^2. \tag{30}$$

These expressions, in particular, the ones for the angular momentum L_z, represent the central result of the work and will be used to analyze certain cases of interaction of the structured light waves with charged particles. Note that up to this point, when the perturbation theory on the wave amplitude a_0 was

presented, the order of this perturbation theory was designated by the upper-right number in round braces. The perturbation theory on a_0 does use Maxwell equations and there are no approximations made for the fields. However, to proceed with certain cases, analytical expressions for the structured light, represented in the next section, are required.

B. Approximate description of a structured electromagnetic wave

As explained in Ref. [13], electromagnetic fields in vacuum can be prescribed via boundary conditions for the transverse electric or magnetic field components. The calculations in this section are presented for the boundary conditions defined for the magnetic field. Similar results may be obtained using the electric field boundary conditions by substitution, $\mathbf{E} \rightarrow -\mathbf{H}$, $\mathbf{H} \rightarrow \mathbf{E}$, which follows from the symmetry of Maxwell equations.

Consider the wave equation for the magnetic field,

$$\left(\Delta - \frac{1}{c^2}\frac{\partial^2}{\partial t^2}\right)\widetilde{\mathbf{H}}(\mathbf{r}, t) = 0, \tag{31}$$

where $\widetilde{\mathbf{E}} = \widetilde{\mathbf{E}}(\mathbf{r}, t)$ and $\widetilde{\mathbf{H}} = \widetilde{\mathbf{H}}(\mathbf{r}, t)$ are the complex representations of $\mathbf{E}$ and $\mathbf{H}$, so that $\mathbf{E} = \mathrm{Re}[\widetilde{\mathbf{E}}]$ and $\mathbf{H} = \mathrm{Re}[\widetilde{\mathbf{H}}]$. With $\xi \equiv t - z/c$ as the new time variable, the wave equation reads

$$\left(\Delta - \frac{2}{c^2}\frac{\partial^2}{\partial\xi\,\partial z}\right)\widetilde{\mathbf{H}}(\mathbf{r}, \xi) = 0. \tag{32}$$

Performing the frequency and transversal Fourier transformations,

$$\widetilde{\mathbf{H}}(\mathbf{r}_\perp, z, \xi) = \int \frac{d\omega\,d\mathbf{k}_\perp}{(2\pi)^3}\mathbf{H}(\omega, \mathbf{k}_\perp, z)e^{i(\omega\xi - \mathbf{k}_\perp \mathbf{r}_\perp)}, \tag{33}$$

where $\mathbf{r}_\perp \equiv x\mathbf{e}_x + y\mathbf{e}_y$, $\mathbf{k}_\perp \equiv k_x\mathbf{e}_x + k_y\mathbf{e}_y$, we obtain that $\mathbf{H}(\omega, \mathbf{k}_\perp, z)$ satisfies

$$\left(\frac{\partial^2}{\partial z^2} - 2i\frac{\omega}{c}\frac{\partial}{\partial z} - \mathbf{k}_\perp^2\right)\mathbf{H}(\omega, \mathbf{k}_\perp, z) = 0. \tag{34}$$

The two independent solutions are forward and backward propagating waves. The forward propagating wave is defined as

$$\mathbf{H}(\omega, \mathbf{k}_\perp, z) = \mathbf{H}(\omega, \mathbf{k}_\perp, 0)e^{i\omega\left(1 - \sqrt{1 - \frac{\mathbf{k}_\perp^2 c^2}{\omega^2}}\right)z/c}, \tag{35}$$

where the condition $\omega^2/c^2 - \mathbf{k}_\perp^2 > 0$, limiting values of the wave vector for the propagating components, arises. The multiplier $\mathbf{H}(\omega, \mathbf{k}_\perp, 0)$ is determined with the boundary condition placed at $z = 0$,

$$\mathbf{H}(\omega, \mathbf{k}_\perp, 0) = \int d\xi\, d\mathbf{r}_\perp \widetilde{\mathbf{H}}\big|_{z=0} e^{-i(\omega\xi - \mathbf{k}_\perp \cdot \mathbf{r}_\perp)},$$
$$\omega^2/c^2 - \mathbf{k}_\perp^2 > 0. \tag{36}$$

The general forward propagating solution reads

$$\widetilde{\mathbf{H}} = \int_{\omega^2/c^2 - \mathbf{k}_\perp^2 > 0} \frac{d\omega\,d\mathbf{k}_\perp}{(2\pi)^3}\mathbf{H}(\omega, \mathbf{k}_\perp, 0)e^{i[\omega\xi - \mathbf{k}_\perp\cdot\mathbf{r}_\perp + (\omega/c - k_z)z]}, \tag{37}$$

where $k_z = \frac{\omega}{c}\sqrt{1 - \frac{\mathbf{k}_\perp^2 c^2}{\omega^2}}$. As it follows from (37), the evanescent components of the boundary condition should be dropped, as long as they produce evanescent parts of the solution. Hence the general forward propagating electric and

magnetic fields may be written in the form [13]

$$\widetilde{\mathbf{E}} = \int \frac{d\omega\,d\mathbf{k}_\perp}{(2\pi)^3}\mathbf{E}(\omega, \mathbf{k}_\perp, 0)e^{i[\omega\xi - \mathbf{k}_\perp\cdot\mathbf{r}_\perp + (\omega/c - k_z)z]},$$
$$\widetilde{\mathbf{H}} = \int \frac{d\omega\,d\mathbf{k}_\perp}{(2\pi)^3}\mathbf{H}(\omega, \mathbf{k}_\perp, 0)e^{i[\omega\xi - \mathbf{k}_\perp\cdot\mathbf{r}_\perp + (\omega/c - k_z)z]}, \tag{38}$$

where explicit specification of the area of integration $\omega^2/c^2 - \mathbf{k}_\perp^2 > 0$ is omitted.

Transverse and longitudinal components of the electric and magnetic fields at focal points are not independent. As independent parameters of the general forward propagating solution, one may choose, e.g., the transverse components of the magnetic field, determined with the boundary condition for the transverse components. The longitudinal component of the magnetic field and the electric field components may be obtained from Maxwell equations, which, in the new variables, read

$$\mathrm{div}\widetilde{\mathbf{H}} = \frac{1}{c}\frac{\partial\widetilde{H}_z}{\partial\xi},$$
$$\mathrm{rot}\widetilde{\mathbf{H}} = \frac{1}{c}\mathbf{e}_z \times \frac{\partial\widetilde{\mathbf{H}}}{\partial\xi} + \frac{1}{c}\frac{\partial\widetilde{\mathbf{E}}}{\partial\xi}, \tag{39}$$

so that

$$H_z(\omega, \mathbf{k}_\perp, 0) = -\frac{\mathbf{k}_\perp \cdot \mathbf{H}_\perp(\omega, \mathbf{k}_\perp, 0)}{k_z},$$
$$\mathbf{E}(\omega, \mathbf{k}_\perp, 0) = -\frac{c\mathbf{k} \times \mathbf{H}(\omega, \mathbf{k}_\perp, 0)}{\omega}. \tag{40}$$

The integration in (38) may be carried out approximately with the expansion of the exponent with the assumption of a slow temporal dependence and slow dependence in the transverse direction,

$$e^{i\omega z/c - i\omega\sqrt{1 - \frac{\mathbf{k}_\perp^2 c^2}{\omega^2}}z/c} = e^{i\frac{\mathbf{k}_\perp^2}{2\omega_0}z}\sum_{n,m}\frac{(\omega - \omega_0)^n \mathbf{k}_\perp^{2m}}{n!\,m!}$$
$$\times \frac{\partial^n}{\partial\omega^n}\frac{\partial^m}{\partial(\mathbf{k}_\perp^2)^m}e^{i\omega\left(1 - \sqrt{1 - \frac{\mathbf{k}_\perp^2 c^2}{\omega^2}} - \frac{c^2\mathbf{k}_\perp^2}{2\omega_0\omega}\right)z/c}\Bigg|_{\substack{\omega=\omega_0 \\ k_\perp=0}}, \tag{41}$$

where ω_0 is the main carrier frequency of the electromagnetic wave. Note that according to the paraxial approximation, one has to consider characteristic values to be $k_\perp \sim w_0^{-1}$, $z \sim w_0^2/\lambda_0$, where w_0 is the beam waist radius and λ_0 is the beam wave length, which means that $ck_\perp^2 z/\omega_0 \sim 1$ and has to be retained in the exponent in (41).

For transversely wide beams with the characteristic beam waist radius w_0, where the characteristic transverse wave vector $k_\perp \sim w_0^{-1}$, the paraxial approximation is defined by expansion on $\frac{\mathbf{k}_\perp^2 c^2}{\omega^2}$, i.e., the order of the paraxial approximation is defined by m; see, e.g., [14]. In this framework, the condition $\omega^2/c^2 - \mathbf{k}_\perp^2$ is neglected in the integration because it leads to exponentially small corrections.

For long enough oscillating waves, considered here and in the case of a slow temporal change of the field amplitude with a characteristic time τ, the condition $\tau \gg 1/\omega_0$ leads to a sharp peak at $\omega = \omega_0$ in the field spectrum. Then, the

approximate expressions for the electromagnetic field may be obtained [15] as an expansion of the factor $e^{i(\omega/c - k_z)z}$ near the peak of the spectrum in (38); the order of the temporal expansion is denoted here by n.

Expansion of the electromagnetic field leads to a series in powers of small parameters related to the inverse beam waist radius $\lambda_0/w_0 \ll 1$ and inverse beam duration $(\omega_0\tau)^{-1} \ll 1$, which may be represented in the form

$$\mathbf{H}(\mathbf{r}, t) = \sum_{\mathbf{n}, m} \mathbf{H}^{\{\mathbf{n}, m\}}(\mathbf{r}, t), \tag{42}$$

where the first (bold) superscript represents the order of the temporal expansion, i.e., the expansion on the inverse beam duration $(\omega_0\tau)^{-1}$, and the second superscript represents the order of the paraxial expansion, i.e., expansion on the inverse beam waist radius λ_0/w_0. In general, temporal and paraxial expansions may be carried out independently, i.e., leaving only $\mathbf{n}$ or only m summation in (42). For the paraxial expansion only, up to the fourth order of $\mathbf{k}_\perp^2$, one obtains

$$e^{i(\omega/c - k_z)z} \approx e^{i\frac{c\mathbf{k}_\perp^2}{2\omega}z}\left(1 + i\frac{c^3\mathbf{k}_\perp^4}{8\omega^3}z + i\frac{c^5\mathbf{k}_\perp^6}{16\omega^5}z + \cdots\right), \tag{43}$$

which corresponds in the used notations to the paraxial expansion,

$$\mathbf{H}(\mathbf{r}, t) = \mathbf{H}^{\{0\}} + \mathbf{H}^{\{1\}} + \mathbf{H}^{\{2\}} + \cdots, \tag{44}$$

where only the second index in (42) is left.

In the same way, the expansion near ω_0, i.e.,

$$e^{i(\omega/c - k_z)z} \approx e^{i\omega_0 z/c - i\omega_0\sqrt{1 - \frac{\mathbf{k}_\perp^2}{\omega_0^2}}\,z/c}$$

$$\times \left\{1 + i\left(1 - \frac{\omega_0}{\sqrt{\omega_0^2 - c^2\mathbf{k}_\perp^2}}\right)\frac{z(\omega - \omega_0)}{c}\right.$$

$$+ \left[\frac{ic^3\mathbf{k}_\perp^2}{z(\omega_0^2 - c^2\mathbf{k}_\perp^2)^{3/2}} - \left(1 - \frac{\omega_0}{\sqrt{\omega_0^2 - c^2\mathbf{k}_\perp^2}}\right)\right]^2$$

$$\left.\times \frac{z^2(\omega - \omega_0)^2}{2c^2} + \cdots\right\}, \tag{45}$$

provides the temporal expansion

$$\mathbf{H}(\mathbf{r}, t) = \mathbf{H}^{\{0\}} + \mathbf{H}^{\{1\}} + \mathbf{H}^{\{2\}} + \cdots. \tag{46}$$

Similar expressions may be presented for the electric field components.

To take into account both the temporal and paraxial corrections in a few low orders, the exponent $e^{i(\omega/c - k_z)z}$ in (38) may be expanded in powers of $\lambda_0/w_0 \ll 1$ and $(\omega_0\tau)^{-1} \ll 1$ as

$$e^{i(\omega/c - k_z)z} \approx e^{i\frac{c\mathbf{k}_\perp^2}{2\omega_0}z}\left[1 + i\frac{c^3\mathbf{k}_\perp^4}{8\omega_0^3}z - i(\omega - \omega_0)\frac{c\mathbf{k}_\perp^2}{2\omega_0^2}z + \cdots\right]. \tag{47}$$

The first term corresponds to the lowest-order paraxial approximation and the constant envelope, the second relates to the first nonvanishing correction to the lowest-order paraxial

approximation with the constant envelope, and the third one corresponds to the temporal corrections taking into account the time variations of the envelope in the lowest-order paraxial approximation. From (40) and (47), one can see that the transverse components of the electromagnetic field are expanded in even powers of λ_0/w_0 and longitudinal in odd powers of λ_0/w_0.

Having in mind the possibility of a general analysis, consider the electromagnetic fields as a linear combination of modes,

$$\mathbf{H} = \sum_i \mathbf{H}^{(i)}, \quad \mathbf{E} = \sum_i \mathbf{E}^{(i)}, \tag{48}$$

which will be later specified for several certain examples. The boundary condition for transverse components in the (x, y) plane is defined for the magnetic field as

$$\mathbf{H}_\perp^{(i)}\big|_{z=0} = \mathbf{H}_{0\perp}^{(i)}(\mathbf{r}_\perp, t), \tag{49}$$

where $z = 0$ is the focal plane. Consider here sufficiently mildly focused beams so that for the chosen $\mathbf{H}_{0\perp}^{(i)}(\mathbf{r}_\perp, t)$, no evanescent components appear.

For the main goal of this work, it is enough to consider the light-particle OAM absorption in the first nonvanishing order of the interaction parameters, defined according to the expansion (42). So, the paraxial approximation $\lambda_0/w_0 \ll 1$ and the approximation of a slowly varying temporal envelope $(\tau\omega_0)^{-1} \ll 1$ are assumed. The boundary conditions in the focal plane are chosen for convenience in the complex form, so that $H_{x,y}^{(i)} = \text{Re}[\widetilde{H}_{x,y}^{(i)}]$:

$$\widetilde{H}_x^{(i)}\big|_{z=0} = E_0 g(t) e^{i\omega_0 t}\mathcal{H}_{0\perp}^{(i)}(\mathbf{r}_\perp),$$
$$\widetilde{H}_y^{(i)}\big|_{z=0} = -i\sigma^{(i)}\widetilde{H}_x^{(i)}\big|_{z=0}, \tag{50}$$

where $g(t)$ is a common slow temporal envelope, E_0 is the common field amplitude, and $\mathcal{H}_{0\perp}^{(i)}(\mathbf{r}_\perp) = \mathcal{H}_{0x}^{(i)}(\mathbf{r}_\perp)\mathbf{e_x} + \mathcal{H}_{0y}^{(i)}(\mathbf{r}_\perp)\mathbf{e_y}$ is an arbitrary function. The used setup (50) represents a superposition of copropagating along the z-axis circularly ($\sigma^{(i)} = \pm 1$) or linearly ($\sigma^{(i)} = 0$) polarized beams.

The function $\mathcal{H}_{0\perp}^{(i)}(\mathbf{r}_\perp)$ may be expressed in terms of the eigenfunctions of the paraxial wave equation u_{pl}, which are defined as [16]

$$u_{\text{pl}}(\mathtt{r}, \varphi, \mathtt{z}) = C_{\text{pl}}\frac{1}{\mathtt{w(z)}}\left(\frac{\mathtt{r}\sqrt{2}}{\mathtt{w(z)}}\right)^{|l|}\exp\left(-\frac{\mathtt{r}^2}{\mathtt{w}^2(\mathtt{z})}\right)L_p^{|l|}\left(\frac{2\mathtt{r}^2}{\mathtt{w}^2(\mathtt{z})}\right)$$

$$\times \exp\left[-il\varphi - i\frac{\mathtt{r}^2\mathtt{z}}{\mathtt{w}^2(\mathtt{z})}\right.$$

$$\left. + i(2p + |l| + 1)\tan^{-1}(\mathtt{z})\right], \tag{51}$$

where $\mathtt{r} = r_\perp/w_0$ and $\mathtt{z} = z/z_R$, with $z_R = \frac{\pi w_0^2}{\lambda_0}$ being the Rayleigh length, are the dimensionless transverse radius and longitudinal coordinate, respectively, $C_{\text{pl}} = \sqrt{\frac{2}{\pi}\frac{p!}{(p+|l|)!}}$ is the normalization constant, $\mathtt{w(z)} = \sqrt{1 + \mathtt{z}^2}$, and $L_p^{|l|}$ is the generalized Laguerre polynomial.

The basis for the boundary conditions is formed by the functions $u_{\text{pl}}(\mathtt{r}, \varphi, \mathtt{z} = 0) \equiv U_{\text{pl}}(\mathtt{r}, \varphi)$. Then the expansion of

$\mathcal{H}_{0\perp}^{(i)}(\mathbf{r}_\perp)$ reads

$$\mathcal{H}_{0\alpha}^{(i)}(r_\perp, \varphi) = \sum_{p=0}^{\infty} \sum_{l=-\infty}^{\infty} a_{pl\alpha}^{(i)} U_{pl}(\mathbf{r}, \varphi), \qquad (52)$$

where

$$a_{pl\alpha}^{(i)} = \int \mathbf{r} d\mathbf{r} d\varphi \mathcal{H}_{0\alpha}^{(i)}(r_\perp, \varphi) U_{pl}^*(\mathbf{r}, \varphi), \qquad (53)$$

and $\alpha = x$ or y.

Substituting the boundary condition (50), expanded in terms of U_{pl}, to (36), integrating over ξ, introducing the angle between $\mathbf{k}_\perp$ and the x axis, such that $\mathbf{k}_\perp \cdot \mathbf{r}_\perp = k_\perp r_\perp \cos(\theta - \varphi)$, and integrating over the azimuthal angle φ, one obtains (A2), using the representation of the Bessel function (A1). There, $g_\omega = \int d\xi g(\xi) e^{-i\omega\xi}$ is the Fourier transform of the envelope. Then, integrating over $\mathbf{r}$ and using the identity (A3), one obtains

$$H_\alpha^{(i)}(\omega, \mathbf{k}_\perp, z=0) = E_0 g_{\omega-\omega_0} \pi w_0^2$$
$$\times \sum_{p,l} a_{pl\alpha}^{(i)} i^{2p+|l|} U_{pl}\left(\frac{k_\perp w_0}{2}, \theta\right). \qquad (54)$$

The lowest-order approximation of the solution then takes the form

$$\widetilde{H}_\alpha^{\{0,0\}} = E_0 g(\xi) \sum_i \sum_{p,l} a_{pl\alpha}^{(i)} u_{pl}(\mathbf{r}, \varphi, \mathbf{z}) e^{i\omega_0\xi}, \qquad (55)$$

where the first (bold) index in $\widetilde{H}_\alpha^{\{0,0\}}$ corresponds to the order of expansion on $(\omega_0\tau)^{-1}$ and the second corresponds to the order of expansion on λ_0/w_0. Introducing

$$\mathcal{H}_\alpha^{\{0,0\}}(\mathbf{r}) = \sum_i \sum_{p,l} a_{pl\alpha}^{(i)} u_{pl}(\mathbf{r}, \varphi, \mathbf{z}), \qquad (56)$$

such that $\mathcal{H}_\alpha^{\{0,0\}}(\mathbf{r})|_{z=0} = \mathcal{H}_{0\alpha}(\mathbf{r}_\perp) \equiv \sum_i \mathcal{H}_{0\alpha}^{(i)}(\mathbf{r}_\perp)$, the lowest-order approximation may be represented in the form

$$\widetilde{\mathbf{H}}_\perp^{\{0,0\}} = E_0 g(\xi) \boldsymbol{\mathcal{H}}_\perp^{\{0,0\}}(\mathbf{r}) e^{i\omega_0\xi}. \qquad (57)$$

The first correction corresponding to the finite pulse duration is

$$\widetilde{\mathbf{H}}_\perp^{\{1,0\}} = \frac{E_0}{\omega_0} g'(\xi) iz \frac{\partial \boldsymbol{\mathcal{H}}_\perp^{\{0,0\}}}{\partial z} e^{i\omega_0\xi}. \qquad (58)$$

As one can see, this correction term is zero at the focal point, which is in agreement with the boundary condition (50).

The first nonvanishing contribution to the longitudinal component of the magnetic field is

$$\widetilde{\mathbf{H}}_\perp^{\{0,1\}} = E_0 g(\xi) \mathcal{H}_z^{\{0,1\}}(\mathbf{r}) e^{i\omega_0\xi}, \qquad (59)$$

where $\mathcal{H}_z^{\{0,1\}} = -i\frac{c}{\omega_0}\nabla_\perp \cdot \boldsymbol{\mathcal{H}}_\perp^{\{0,0\}}$. The first nonvanishing correction to the transverse components corresponding to the paraxial approximation is

$$\widetilde{\mathbf{H}}_\perp^{\{0,2\}} = \frac{cE_0}{\omega_0} g(\xi) \frac{z}{2i} \frac{\partial^2 \boldsymbol{\mathcal{H}}_\perp^{\{0,0\}}}{\partial z^2} e^{i\omega_0\xi}, \qquad (60)$$

which is zero at the focal point. The next corrections and expressions for the electric field components are presented in the Appendix 2.

In what follows, the general approximate expressions are presented for the momentum, energy, and orbital angular momentum (OAM), absorbed by uniformly distributed electrons from the mildly focused laser pulse of a subrelativistic intensity. These general expressions are derived in the frames of the perturbation theory developed on the field amplitude a_0, the paraxial parameter λ_0/w_0, and the adiabatic parameter of the laser pulse $(\omega_0\tau)^{-1}$, aiming the accurate consideration of the main nonvanishing contributions. The calculations show that for the OAM absorption, it is enough to consider the fourth order on a_0, the first order on $(\omega_0\tau)^{-1}$ (the first correction to the main order), and the main order of the paraxial approximation.

C. Analytical estimates for the energy, momentum, and angular momentum gained by a particle in a structured wave

As shown below, the first-order temporal correction provides a contribution to the average angular momentum gain by electrons of the same order as the constant amplitude approximation, and hence should be considered in the calculations to obtain a correct expression for the average angular momentum gain. The magnetic field accounting for the first-order temporal correction may be represented, according to (45) and (58), as

$$\mathbf{H} = E_0 \mathrm{Re}\left\{\left[g(t-z/c)\boldsymbol{\mathcal{H}}^{\{0\}}(\mathbf{r})\right.\right.$$
$$\left.\left. + \frac{1}{\omega_0} g'(t-z/c)\boldsymbol{\mathcal{H}}^{\{1\}}(\mathbf{r})\right] e^{i\omega_0(t-z/c)}\right\}, \qquad (61)$$

where both $\boldsymbol{\mathcal{H}}^{\{0\}}$ and $\boldsymbol{\mathcal{H}}^{\{1\}}$ are calculated with a desired accuracy on the paraxial parameter λ_0/w_0. The derivative of the envelope $g'(t-z/c)$ may be estimated as $g' \sim \frac{g}{\omega_0\tau} \ll g$, which makes this term a small correction to the leading one. In addition, this condition means that $g(t-z/c)$ is a smooth function, compared to $e^{i\omega_0(t-z/c)}$, and we also consider $g'(t-z/c)$ to be a smooth function as well.

The spatial amplitude $\boldsymbol{\mathcal{H}}^{\{0\}}$ is defined from the boundary condition (50). The lowest-order paraxial approximation for the transverse components is (56) and the lowest-order paraxial approximation for the transverse components of $\boldsymbol{\mathcal{H}}^{\{1\}}(\mathbf{r})$ is defined as (58).

The electric field may be written in a similar form as (61),

$$\mathbf{E} = E_0 \mathrm{Re}\left\{\left[g(t-z/c)\boldsymbol{\mathcal{E}}^{\{0\}}(\mathbf{r})\right.\right.$$
$$\left.\left. + \frac{1}{\omega_0} g'(t-z/c)\boldsymbol{\mathcal{E}}^{\{1\}}(\mathbf{r})\right] e^{i\omega_0(t-z/c)}\right\}, \qquad (62)$$

where $\boldsymbol{\mathcal{E}}^{\{0\}}$ and $\boldsymbol{\mathcal{E}}^{\{1\}}$ are the spatial amplitudes, defined from the amplitudes of the magnetic field, which in a few lowest orders of paraxial approximation are given by

$$\mathcal{E}_x^{\{0,0\}}(\mathbf{r}) = \mathcal{H}_y^{\{0,0\}}(\mathbf{r}),$$
$$\mathcal{E}_y^{\{0,0\}}(\mathbf{r}) = -\mathcal{H}_x^{\{0,0\}}(\mathbf{r}),$$
$$\boldsymbol{\mathcal{E}}_\perp^{\{1,0\}}(\mathbf{r}) = iz\frac{\partial \boldsymbol{\mathcal{E}}_\perp^{\{0,0\}}(\mathbf{r})}{\partial z}; \qquad (63)$$

see more details in the Appendix.

Substituting (62) into (30), in the main order of the slowly varying envelope approximation, one obtains

$$\mathbf{p}^{(2)}(t_\infty) = -m_e c^2 \frac{a_0^2}{4} \nabla_0 |\boldsymbol{\mathcal{E}}^{\{0\}}|^2 \tau_{\text{int}},$$

$$L_z^{(2)}(t_\infty) = -m_e c^2 \frac{a_0^2}{4} \frac{\partial}{\partial \varphi_0} |\boldsymbol{\mathcal{E}}^{\{0\}}|^2 \tau_{\text{int}},$$

$$\varepsilon^{(4)}(t_\infty) = m_e c^4 \frac{a_0^4}{32} \left(\nabla_0 |\boldsymbol{\mathcal{E}}^{\{0\}}|^2 \right)^2 \tau_{\text{int}}^2, \qquad (64)$$

where $\tau_{\text{int}} \equiv \int_{-\infty}^{\infty} g^2(t) dt \sim \tau$ is the characteristic time of the interaction.

In order to calculate the average gained angular momentum in the fourth order, one has to calculate $\mathbf{r}^{(2)}$ and $L_z^{(2)}$ after the interaction with the laser. The lowest order of $\mathbf{r}^{(2)}$ arises from the second term in (15). At infinite time, it diverges into infinity and should be regularized. The regularization may be obtained by setting the last moment of time to be T, assuming $T \to \infty$ at the end of the calculations. Substituting the first term of (62) and evaluating $\mathbf{r}^{(2)}$ at high values of time T, one obtains

$$\mathbf{r}^{(2)}(T) \approx -c^2 \frac{a_0^2}{4} \nabla_0 |\boldsymbol{\mathcal{E}}^{\{0\}}|^2 \int_{-\infty}^{T} dt \int_{-\infty}^{t} g^2(t') dt'. \qquad (65)$$

The corresponding contribution to the average angular momentum is

$$\langle L_z^{(4)}(T) \rangle_{\varphi_0} \approx m_e c^4 \frac{a_0^4}{32} \left\langle \frac{\partial}{\partial \varphi_0} \left(\nabla_0 |\boldsymbol{\mathcal{E}}^{\{0\}}|^2 \right)^2 \right\rangle_{\varphi_0}$$

$$\times \tau_{\text{int}} \int_{-\infty}^{T} dt \int_{-\infty}^{t} g^2(t') dt' = 0, \qquad (66)$$

which is a partial derivative with respect to φ_0 and vanishes, being averaged with the isotropic distribution function. This

expression does not depend on T and the limit $T \to \infty$ may be applied.

The next contribution to the average angular momentum gain results from both terms in $\mathbf{r}^{(2)}$ in (15). The first one may be evaluated in the lowest order. In the second term, one has to consider the correction to the slowly varying envelope approximation.

The first term in the lowest-order expansion in powers of $(\omega_0 \tau)^{-1}$ reads

$$\int_{-\infty}^{\infty} dt' [\mathbf{r}^{(1)}(t') \cdot \nabla_0] \mathbf{v}^{(1)}(t')$$

$$\approx \frac{c^2}{\omega_0} \frac{a_0^2}{2} \text{Re} \left[i(\boldsymbol{\mathcal{E}}^{\{0\}*} \cdot \nabla_0) \boldsymbol{\mathcal{E}}^{\{0\}} + \mathcal{E}_z^{\{0\}} \boldsymbol{\mathcal{E}}^{\{0\}*} \right] \tau_{\text{int}}$$

$$\approx -\frac{c^2}{\omega_0} \frac{a_0^2}{2} \frac{\partial}{\partial x_{0j}} \text{Re} \left(i \mathcal{E}_j^{\{0\}} \boldsymbol{\mathcal{E}}^{\{0\}*} \right) \tau_{\text{int}}, \qquad (67)$$

where $(\nabla \cdot \boldsymbol{\mathcal{E}}^{\{0\}}) \approx i \mathcal{E}_z^{\{0\}}$ in the lowest order was used.

The second term consists of two parts: the first one arises from the action of ∇_0 on $g(t - z_0/c)$, and the second one from the correction to the slowly varying envelope approximation. This results in the following two contributions to $\mathbf{r}^{(2)}$, correspondingly:

$$c \frac{a_0^2}{4} |\boldsymbol{\mathcal{E}}^{\{0\}}|^2 \tau_{\text{int}} \mathbf{e}_z \qquad (68)$$

and

$$-\frac{c^2}{\omega_0} \frac{a_0^2}{8} \nabla_0 \text{Re}(\boldsymbol{\mathcal{E}}^{\{0\}} \boldsymbol{\mathcal{E}}^{\{1\}*}) \tau_{\text{int}}. \qquad (69)$$

Collecting the three terms (67)–(69) together, substituting to the expression (27) for $\langle L_z^{(4)} \rangle_{\varphi_0}$, and integrating the first two of them by parts inside the averaging, one obtains

$$\langle L_z^{(4)}(t_\infty) \rangle_{\varphi_0} = \frac{m_e c^4}{\omega_0} \frac{a_0^4}{8} \left\langle \left(\left\{ \frac{1}{4} \left[\nabla_0 \text{Re}(\boldsymbol{\mathcal{E}}^{\{0\}} \boldsymbol{\mathcal{E}}^{\{1\}*}) \cdot \nabla_0 \right] + \frac{\omega_0}{2c} \frac{\partial |\boldsymbol{\mathcal{E}}^{\{0\}}|^2}{\partial z_0} \right\} \frac{\partial |\boldsymbol{\mathcal{E}}^{\{0\}}|^2}{\partial \varphi_0} + \frac{\partial}{\partial x_{0k}} \left[\frac{\partial}{\partial x_{0j}} \text{Re}\left(i\mathcal{E}_j^{\{0\}} \mathcal{E}_k^{\{0\}*}\right) \frac{\partial |\boldsymbol{\mathcal{E}}^{\{0\}}|^2}{\partial \varphi_0} \right] \right) \right\rangle_{\varphi_0} \tau_{\text{int}}^2. \qquad (70)$$

For a Laguerre-Gaussian beam with a characteristic transverse size w_0 and the longitudinal size $z_R \sim w_0^2/\lambda_0$, the expressions (64) and (70) may be estimated in the main orders as

$$\left| \mathbf{p}_\perp^{(2)}(t_\infty) \right| \sim m_e c^2 \frac{a_0^2 \tau_{\text{int}}}{w_0},$$

$$p_z^{(2)}(t_\infty) \sim \frac{m_e c^3}{\omega_0} \frac{a_0^2 \tau_{\text{int}}}{w_0^2},$$

$$L_z^{(2)}(t_\infty) \sim m_e c^2 a_0^2 \tau_{\text{int}},$$

$$\varepsilon^{(4)}(t_\infty) \sim m_e c^4 \frac{a_0^4 \tau_{\text{int}}^2}{w_0^2},$$

$$\langle L_z^{(4)}(t_\infty) \rangle_{\varphi_0} \sim \frac{m_e c^4}{\omega_0} \frac{a_0^4 \tau_{\text{int}}^2}{w_0^2}. \qquad (71)$$

Note that the transverse and the longitudinal characteristic sizes are different, which makes the estimations for transverse and longitudinal momenta also be different.

The higher orders of the perturbation theory have the $\sim \tau_{\text{int}}^2$ dependence, meaning formally that for later interaction times the energy and OAM transfer become more efficient. These estimates, however, actually require that the fourth-order terms are less than the second-order ones or, using the expressions for $\langle L_z^{(4)}(t_\infty) \rangle_{\varphi_0}$ and $L_z^{(2)}(t_\infty)$, that $a_0^2 \tau_{\text{int}}/w_0^2 \ll \omega_0/c^2$. This means that for long pulses, for which $\tau_{\text{int}} \gtrsim \omega_0 w_0^2/c^2 a_0^2$, after the moment of time $t \sim \omega_0 w_0^2/c^2 a_0^2$, the perturbation theory fails. The obtained limitation for the interaction time may be rewritten as $\omega_0 \tau_{\text{int}} \ll (w_0/l_{osc})^2$, where $l_{osc} = a_0 \lambda_0$ is the characteristic oscillation amplitude of the electron in the wave.

Comparing the second- and the fourth-order expressions for the transferred momentum in (71), one can see that

$l_{osc}^2 \omega_0 \tau_{\text{int}}/w_0^2$ is the actual perturbation theory parameter for the expansion of gained electron values, which counts for both the paraxial approximation and the slow-varying envelope approximation, and means that the field amplitude a_0 may actually be not too small for the applicability of the obtained results. This is confirmed by the examples presented in the next section.

According to the arguments provided directly above, although the perturbation theory was developed under the formal assumption of a low-amplitude a_0, a moderate intensity regime of the interaction $a_0 \sim 1$ is considered in the following. At field amplitudes $a_0 \sim 1$, the following estimates may be obtained:

$$p_z^{(2)}(t_\infty) \sim \frac{m_e c^3}{\omega_0} \frac{\tau_{\text{int}}}{w_0^2},$$

$$\varepsilon^{(4)}(t_\infty) \sim m_e c^4 \frac{\tau_{\text{int}}^2}{w_0^2},$$

$$(p_z - \varepsilon/c)\big|_{t_\infty} \sim \frac{m_e c^3}{\omega_0} \frac{\tau_{\text{int}}}{w_0^2}, \tag{72}$$

where the first two are the consequence of (71) and the last one does not depend on perturbation theory and may be obtained from the analysis of integrals of motion. As shown in Ref. [6], the growth rate of $(p_z - \varepsilon/c)$ is proportional to the field amplitude and inversely proportional to the square of the beam waist, which in the notations of this work corresponds to the third estimate in (72). This is a consequence of the weak dependence of the waves in the paraxial approximation on z, which in the limiting case of plane waves leads to the conservation of a quantity $(p_z - \varepsilon/c)$, which becomes an integral of motion. According to (72) in this regime,

$$(p_z - \varepsilon/c)\big|_{t_\infty} \sim p_z^{(2)}\big|_{t_\infty}. \tag{73}$$

To make the analysis consistent, the energy scaling in (73) should not be greater than that for the momentum, which is an omen that higher orders of perturbation theory should be considered for p_z in this regime. Indeed, in the frameworks of the paraxial and slowly varying temporal approximation for the discussed parameters, the leading term in the expression for the fourth-order longitudinal momentum (25) may be estimated as $\sim m_e c^3 \tau_{\text{int}}^2/w_0^2$ and has the form

$$p_z^{(4)}(t_\infty) = -\frac{m_e}{2} \int_{-\infty}^{\infty} \frac{\partial}{\partial z_0} [\mathbf{v}^{(2)}(t)]^2 dt, \tag{74}$$

which, after substitution of (62), becomes

$$p_z^{(4)}(t_\infty) = \varepsilon^{(4)}(t_\infty)/c, \tag{75}$$

due to the presence of z in the envelope function $g(t - z/c)$. Expression (75) corresponds to the integral of motion $p_z - \varepsilon/c$ for a charged particle in a plane wave.

As a result, the estimated from the analytical theory values of the gained momentum, energy, and angular momentum for $a_0 \sim 1$ take the form

$$\mathbf{p}_{\perp,\text{theor}} = \mathbf{p}_\perp^{(2)}, \quad p_{z,\text{theor}} = p_z^{(2)} + \varepsilon^{(4)}/c, \quad L_{z,\text{theor}} = L_z^{(2)},$$

$$\langle L_{z,\text{theor}} \rangle_{\varphi_0} = \langle L_z^{(4)} \rangle_{\varphi_0}, \quad \varepsilon_{\text{theor}} = \varepsilon^{(4)}, \tag{76}$$

where all the values are taken after the interaction at t_∞ and $\perp$ stands for the transverse components of the vectors. It is possible that these expressions turn to zero at some laser field configurations. In these cases, higher orders of the perturbation theory or electromagnetic field expansions are required. However, configurations with nonzero values of these expressions definitely exist and will be presented further.

III. SOME EXAMPLES FOR CERTAIN POLARIZATION CASES

A. Circular polarization, one LG mode

Consider a circularly polarized Laguerre-Gaussian (LG) beam, $\sigma = \pm 1$. Boundary conditions (50) take the form

$$\widetilde{H}_x\big|_{z=0} = E_0 g(t) e^{i\omega_0 t} \frac{u_{\text{pl}}}{\sqrt{2}}\bigg|_{z=0},$$

$$\widetilde{H}_y\big|_{z=0} = -i\sigma \widetilde{H}_x\big|_{z=0}. \tag{77}$$

As long as u_{pl} depends on φ as $\sim e^{-il\varphi}$, the boundary condition depends on φ as $\widetilde{H}_y|_{z=0} = -i\sigma \widetilde{H}_x|_{z=0} \sim e^{-il\varphi}$. These relations between the components of the electromagnetic field apply to the solution of Maxwell equations in the whole space, i.e., for the solution in the whole space, $\widetilde{H}_y = -i\sigma \widetilde{H}_x \sim e^{-il\varphi}$. This leads to the following dependence of the exact solution on φ in cylindrical coordinates:

$$\widetilde{H}_r \sim e^{-i(l+\sigma)\varphi},$$

$$\widetilde{H}_\varphi = -i\sigma \widetilde{H}_r \sim e^{-i(l+\sigma)\varphi},$$

$$\widetilde{H}_z \sim e^{-i(l+\sigma)\varphi}. \tag{78}$$

Hence, the components of $\boldsymbol{\mathcal{E}}^{\{0\}}$ of the electric field (62) are $\mathcal{E}_r^{\{0\}} \sim \mathcal{E}_\varphi^{\{0\}} \sim \mathcal{E}_z^{\{0\}} \sim e^{-i(l+\sigma)\varphi}$ and $\frac{\partial |\boldsymbol{\mathcal{E}}^{\{0\}}|^2}{\partial \varphi_0} = 0$. Substituting this into (70), one obtains $\langle L_z^{(4)}(t_\infty)\rangle_{\varphi_0} = 0$, which means that the angular momentum, on average, is not transferred to electrons in the considered orders of the perturbation theory and the paraxial and slowly varying temporal envelope approximations.

B. Linear polarization, one LG mode

Consider a linearly polarized Laguerre-Gaussian beam, $\sigma = 0$. The boundary condition (50) takes the form

$$\widetilde{H}_x\big|_{z=0} = E_0 g(t) e^{i\omega_0 t} u_{\text{pl}}\big|_{z=0},$$

$$\widetilde{H}_y\big|_{z=0} = 0. \tag{79}$$

In the lowest order of the paraxial approximation, $\frac{\partial |\boldsymbol{\mathcal{E}}^{\{0,0\}}|^2}{\partial \varphi_0} = 0$, and the angular momentum, on average, is not transferred to electrons in the considered orders of approximations.

C. Linear polarization, superposition of LG modes

Probably one of the most efficient angular momentum transfers occurs in the electromagnetic fields represented by a superposition of Laguerre-Gaussian modes with different azimuthal indexes. It provides a nonzero average gain of the angular momentum already in the lowest orders of the approximations considered in this work.
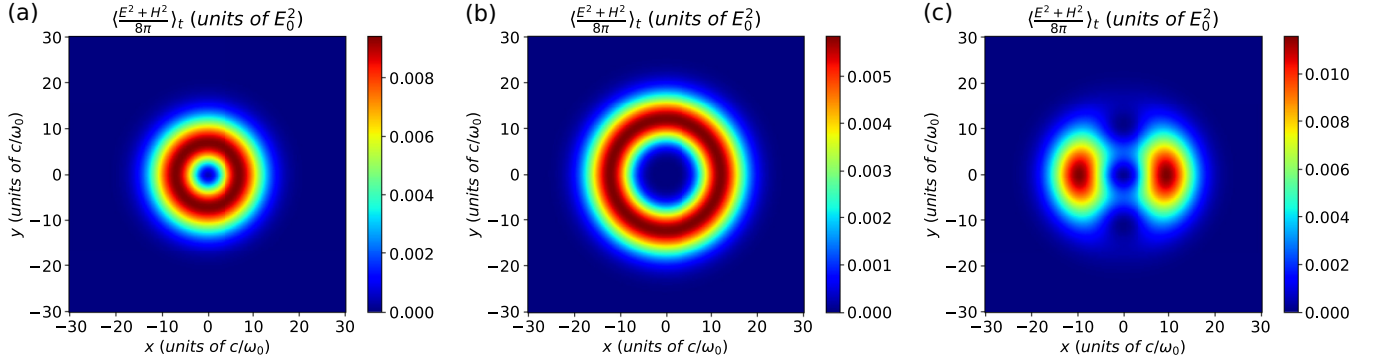
FIG. 2. Distribution of the energy density of a linearly polarized wave for (a) one LG mode with $p = 0$, $l = 1$, (b) one LG mode with $p = 0$, $l = 3$, and (c) superposition of two LG modes with $p = 0$, $l = 1$ and $q = 0$, $m = 3$ in the focal plane.

For a superposition of Laguerre-Gaussian modes with different azimuthal indexes, the energy density, averaged over the laser period, is asymmetric with respect to the laser axis in the case of superposition of LG modes with different azimuthal indexes; see Fig. 2, which shows the averaged energy density for monochromatic waves [$g(t) = 1$]. This asymmetry is responsible for a more efficient OAM transfer.

Note that in experiment, particularly in a high-intensity regime, it may appear challenging to obtain a pure single Laguerre-Gaussian mode [17–19]. A set of secondary modes may additionally be exited, so that the resulting wave actually represents a superposition of Laguerre-Gaussian modes with different numbers (p, l).

Consider the case of linear polarization $\sigma = 0$, and a superposition of Laguerre-Gaussian beams with azimuthal indexes l and m. The boundary conditions (50) then may be written as

$$\widetilde{H}_x\big|_{z=0} = E_0 g(t) e^{i\omega_0 t} \frac{u_{\mathrm{pl}} + u_{\mathrm{qm}}}{\sqrt{2}}\bigg|_{z=0}, \quad \widetilde{H}_y\big|_{z=0} = 0, \quad (80)$$

and in the lowest orders of the used approximations,

$$\mathcal{E}^{\{0,0\}} = \frac{u_{\mathrm{pl}} + u_{\mathrm{qm}}}{\sqrt{2}} \mathbf{e}_x. \quad (81)$$

A single particle gains an angular momentum

$$L_z^{(2)}(t_\infty) = -m_e c^2 \frac{a_0^2}{4}(l - m)\mathrm{Re}(i u_{\mathrm{pl}}^* u_{\mathrm{qm}})\tau_{\mathrm{int}}. \quad (82)$$

From this expression, the extreme values of the gained angular momentum are

$$L_{z,\mathrm{extr}}^{(2)}(t_\infty) = \pm m_e c^2 \frac{a_0^2}{4}(l - m)\big|u_{\mathrm{pl}} u_{\mathrm{qm}}\big|\bigg|_{\varphi_0=0}\tau_{\mathrm{int}}. \quad (83)$$

The expression for the average gained angular momentum reads, after integration over φ_0,

$$\left\langle L_z^{(4)}(t_\infty)\right\rangle_{\varphi_0} = -\frac{m_e c^4}{\omega_0}(l - m)\frac{a_0^4}{64}\mathrm{Re}\left[i\left(\frac{\partial A}{\partial r_0}\frac{\partial B^*}{\partial r_0} + \frac{(l-m)^2}{r_0^2}AB^* + 2A\frac{\partial A^*}{\partial z_0}\right)\right]\tau_{\mathrm{int}}^2, \quad (84)$$

where $A = u_{\mathrm{qm}}^* u_{\mathrm{pl}}|_{\varphi_0=0}$ and $B = \frac{i z_0}{2}(u_{\mathrm{qm}}^* \frac{\partial u_{\mathrm{pl}}}{\partial z_0} - u_{\mathrm{pl}}\frac{\partial u_{\mathrm{qm}}^*}{\partial z_0})|_{\varphi_0=0}$. The average gained energy and longitudinal momentum read

$$\left\langle \varepsilon^{(4)}(t_\infty)\right\rangle_{\varphi_0} = m_e c^4 \frac{a_0^4}{128}\left[\left(\frac{\partial |u_{\mathrm{pl}}|^2}{\partial r_0} + \frac{\partial |u_{\mathrm{qm}}|^2}{\partial r_0}\right)^2 + 2\left|\frac{\partial (u_{\mathrm{pl}} u_{\mathrm{qm}}^*)}{\partial r_0}\right|^2\right]\bigg|_{\varphi_0=0}\tau_{\mathrm{int}}^2, \quad l \neq m, \quad (85)$$

$$\left\langle p_z^{(2)}(t_\infty)\right\rangle_{\varphi_0} = -\frac{m_e c^3}{\omega_0}\frac{a_0^2}{8}\frac{\partial(|u_{\mathrm{pl}}|^2 + |u_{\mathrm{qm}}|^2)}{\partial z_0}\bigg|_{\varphi_0=0}\tau_{\mathrm{int}}. \quad (86)$$

Consider the following special cases:

(a) One can see that when $l = m$, the angular momentum is not transferred in the used orders of approximations.

(b) If $p = q$, $m = -l$, then both A and B become real and the average angular momentum turns to zero. It is a natural result since such an electromagnetic field configuration does not carry an angular momentum.

(c) If one changes the azimuthal indexes (l, m) to $(-l, -m)$, one can see that both A and B do not change, and the average gained angular momentum changes its sign which is also expected, because the OAM of the field also changes its sign.

To compare the obtained analytical estimates with numerical results, which may, with a limited numerical accuracy, provide both the electromagnetic fields and the angular momentum gained by particles beyond the perturbation theory limitations, the interaction of electrons with electromagnetic fields was studied with the PIC code SMILEI [20] in cylindrical geometry. To focus on the single-particle effects, the interaction between the electrons was not calculated. The
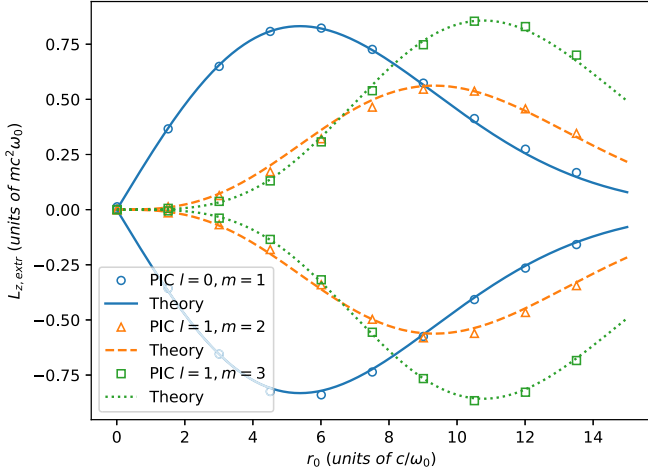
FIG. 3. Extreme values of gained angular momentum after the interaction with $l = 0$, $m = 1$ (blue solid), $l = 1$, $m = 2$ (orange dashed), $l = 1$, $m = 3$ (green dotted) beams as a function of initial distance of the particle from the beam axis. Dots, triangles, and squares represent PIC numerical results; lines represent predictions of the model for the corresponding beam configurations.

use of the PIC code allows one to optimize the simulation time and, more importantly, obtain the numerically calculated fields, which contain all the paraxial and temporal corrections.

In simulations, the numerical box consisted of 6000 cells in the longitudinal direction and 1600 in the radial direction with spatial resolution of 2.5 nm. The laser field was injected from $z = 0$ boundary, with conditions (80) placed at the boundary. The carrier laser frequency was $\omega_0 = 2.3 \times 10^{15}$ s^{-1}, the beam waist radius was as small as $w_0 = 1.3$ μm to increase the observed value of the transferred OAM and limit the size of the simulation box, and the duration of the laser pulse, $\tau = 2\pi n/\omega_0$, where $n = 6$ is the number of periods. The dimensionless intensity used in the simulations was $a_0 = 1$, the radial indexes were $p = q = 0$, and three cases for the azimuthal numbers were considered: $l = 0$, $m = 1$; $l = 1$, $m = 2$; and $l = 1$, $m = 3$. The common temporal envelope is chosen to be $g(t) = \cos^2(\frac{t-\tau/2}{\tau}\pi)$ when $|t - \tau/2| < \tau/2$, and 0 otherwise. In this case, $\tau_{\text{int}} = \frac{3}{8}\tau$. Absorbing boundary conditions were set for the electromagnetic fields on all boundaries, excluding the injection boundary $z = 0$. For better statistics, with a numerically feasible number of particles, electrons were initialized at 2.5 μm from the laser injection plane at given radial distances, but with different randomly distributed angles; the number of particles for each radial distance N_{r_0} was about 2×10^5. These distances were defined as a set of 10 fixed values from $r_0 = 0$ to $r_0 = 1.9$ μm inside a thin disk with the axis being that of the laser beam.

Figure 3 represents the extreme values of the gained angular momentum after the interaction with three different beam configurations; the points are numerical results and the lines are drawn according to (83). The vertical axis corresponds to the maximum and minimum extreme values of the angular momentum, gained by particles, while the horizontal axis corresponds to the initial radial distance of the particles from the beam axis.

As long as the maximum local intensity of a Laguerre-Gaussian beam increases with the growth of the azimuthal index and its position shifts to larger radial distances, the maximum of the extreme value of the gained angular momentum also shifts toward the higher values of the initial distance from the beam axis with the growth of the azimuthal index.

The average angular momentum transfer is an effect of the fourth-order perturbation theory, while the extreme values of the gained angular momentum, indicating single-particle gain, appear to be nonzero already in the second order. This leads to substantial statistical errors in the calculations of the average angular momentum gain, even when using a large amount of particles in the simulations. The average angular momentum, gained by the particles in the numerical simulations, was calculated according to the following procedure:

$$\overline{L_z}(r_0) \equiv \frac{\sum_{i=1}^{N_{r_0}} L_{z,i}}{N_{r_0}}, \tag{87}$$

where $L_{z,i}$ is the gained angular momentum of the ith particle, which initial distance from the beam axis lies in the interval $[r_0, r_0 + \Delta r_0]$ and N_{r_0} is the number of particles with initial coordinates in this interval. The error was estimated according to the central limit theorem,

$$|\overline{L_z} - \langle L_z \rangle_{\varphi_0}| \sim \frac{\sqrt{\langle (L_z - \langle L_z \rangle_{\varphi_0})^2 \rangle_{\varphi_0}}}{\sqrt{N}}, \tag{88}$$

where $\overline{L_z}$ stands for averaging over the ensemble of the particles in the numerical simulations and $\langle \cdot \rangle_{\varphi_0}$ for the averaging over analytical expressions.

As long as $\langle (L_z - \langle L_z \rangle_{\varphi_0})^2 \rangle_{\varphi_0} = \langle L_z^2 \rangle_{\varphi_0} - \langle L_z \rangle_{\varphi_0}^2 < \langle L_z^2 \rangle_{\varphi_0}$ and $\langle L_z \rangle_{\varphi_0}$ is of the fourth order and therefore may be considered negligible here compared to $\langle L_z^2 \rangle_{\varphi_0}^{1/2}$, the right-hand side may be estimated as

$$\sqrt{\langle (L_z - \langle L_z \rangle_{\varphi_0})^2 \rangle_{\varphi_0}/N} \sim \sqrt{\langle (L_z^{(2)})^2 \rangle_{\varphi_0}/N}$$

$$\sim |L_{z,\text{extr}}^{(2)}(t_\infty)|/\sqrt{N} \sim m_e c^2 a_0^2 \tau_{\text{int}}/\sqrt{N}. \tag{89}$$

The relative statistical error may then be estimated as

$$\frac{\sqrt{\langle (L_z - \langle L_z \rangle_{\varphi_0})^2 \rangle_{\varphi_0}/N}}{|\langle L_z^{(4)} \rangle_{\varphi_0}|} \sim \frac{\omega_0}{c^2} \frac{w_0^2}{a_0^2 \tau_{\text{int}} \sqrt{N}}, \tag{90}$$

which rises when amplitude a_0 decreases. In the simulation results shown below, these errors are not always shown to make the plots readable, though their values are sometimes considerable. The exemplary plot in Fig. 4 demonstrates the scale of the error bars for the case $l = 1$, $m = 3$. The amounts of the quantities averaged over the initial azimuthal angle gained by electrons, such as the energy, the longitudinal, and the angular momentum versus their initial radial distance from the axis of the laser beam, are shown in Figs. 5–8.

The presented plots demonstrate that the perturbation theory allows a semiquantitative description for the angular momentum gain by particles even at relatively high intensities, i.e., when $a_0 \sim 1$. As explained in the previous section, the reason for this is probably that the beam waist is large enough, i.e., $2\pi w_0/\lambda_0 \gg 1$.
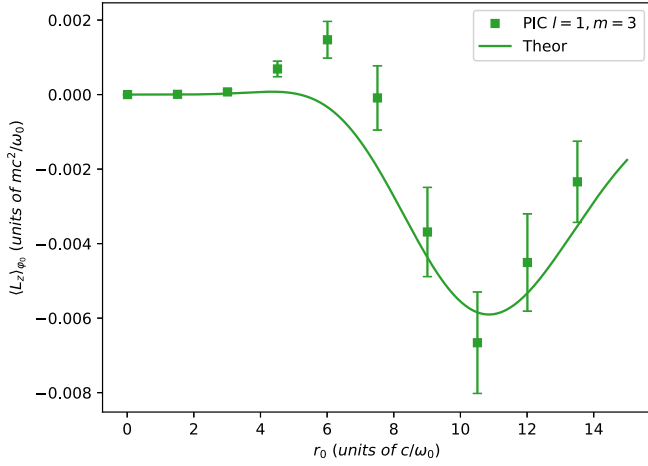
FIG. 4. Average angular momentum, gained by electrons after the interaction with the $l = 1$, $m = 3$ beam, as a function of initial distance of the particle from the beam axis. Squares represent PIC numerical results, the line represents predictions of the model, and the vertical lines represent the value of the statistical error.

IV. DISCUSSION

As the presented analysis of the angular momentum transfer shows, three parameters of the interaction are essential: dimensionless field amplitude a_0, relation of the period of laser oscillations to the laser pulse duration $(\omega_0 \tau)^{-1}$, and the relation of the laser wavelength to the laser beam waist radius, λ_0 / w_0. In this work, all three parameters are considered as being small, i.e., $a_0 \ll 1$, $(\omega_0 \tau)^{-1} \ll 1$ and $\lambda_0 / w_0 \ll 1$, which allows one to develop the perturbation theory based on expansion of the calculated values in powers of these small parameters. The relations between the parameters are not discussed, as the solutions are obtained in the lowest orders, which may provide a nonzero result. However, in
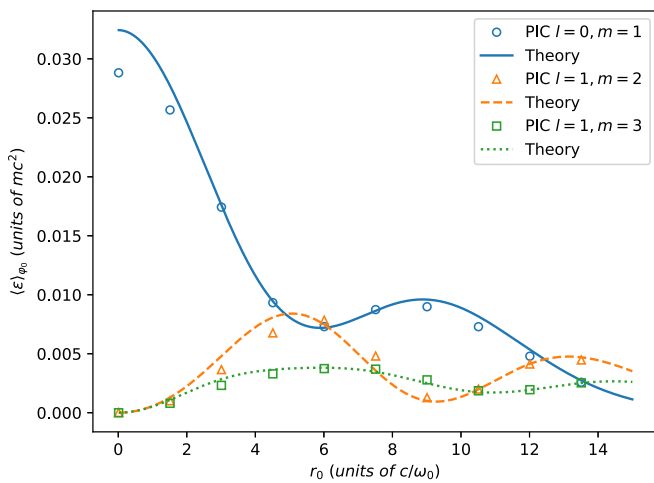

FIG. 6. Average longitudinal momentum, gained by electrons after the interaction with $l = 0$, $m = 1$ (blue solid), $l = 1$, $m = 2$ (orange dashed), $l = 1$, $m = 3$ (green dotted) beams as a function of initial distance of the particle from the beam axis. Dots, triangles, and squares represent PIC numerical results; lines represent predic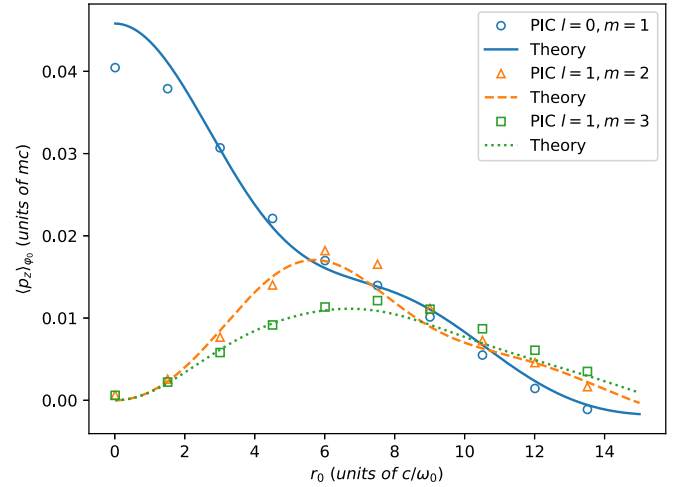tions of the model for the corresponding beam configurations, accounting for the second- and fourth-order perturbation theory.

general, especially when the considered approximation gives a zero gained orbital momentum, e.g., the considered case of a single linearly polarized Laguerre-Gaussian beam may require further expansion in $(\omega_0 \tau)^{-1}$ or λ_0 / w_0, depending on the relation between these parameters.

It is interesting to note, once again, that according to the estimates (71), the obtained expansion actually develops on the combination of these parameters, which at the same time takes into account the amplitude of the field, the beam waist, and the temporal behavior. The combination is the relation of the particle oscillation amplitude squared to the beam waist
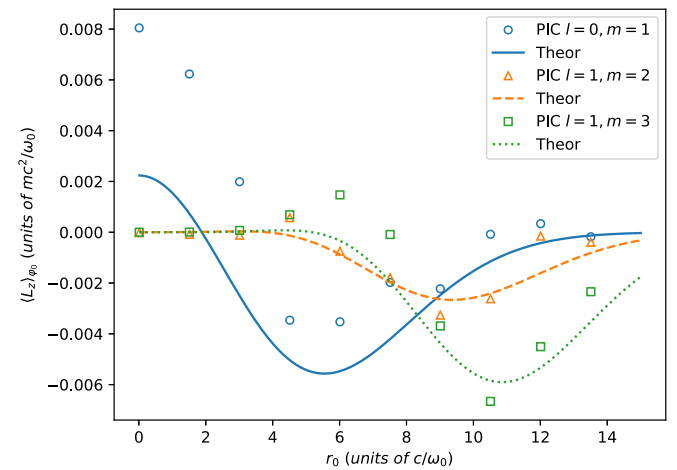

FIG. 5. Average kinetic energy, gained by electrons after the interaction with $l = 0$, $m = 1$ (blue solid), $l = 1$, $m = 2$ (orange dashed), $l = 1$, $m = 3$ (green dotted) beams as a function of the initial distance of the particle from the beam axis. Dots, triangles, and squares represent PIC numerical results; lines represent predictions of the model for the corresponding beam configurations.

FIG. 7. Average angular momentum, gained by electrons after the interaction with $l = 0$, $m = 1$ (blue solid), $l = 1$, $m = 2$ (orange dashed), $l = 1$, $m = 3$ (green dotted) beams as a function of initial distance of the particle from the beam axis. Dots, triangles, and squares represent PIC numerical results; lines represent predictions of the model for the corresponding beam configurations.
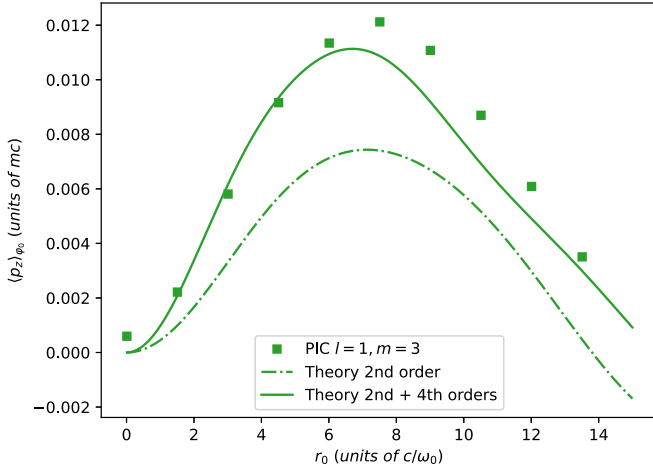
FIG. 8. Average longitudinal momentum, gained by electrons after the interaction with the $l = 1$, $m = 3$ beam as a function of initial distance of the particle from the beam axis. Squares represent PIC numerical results; the solid line represents predictions of the model, accounting for the second- and the fourth-order perturbation theory. The dash-dotted line represents predictions of the model, accounting only for the second-order perturbation theory.

radius squared and multiplied be the duration of the beam. This allows one to consider, as a result, the mild-relativistic values of $a_0 \sim 1$ and obtain a good semiquantitative agreement between the analytical and the numerical results. It is also important that the approximations that are used are not suitable for short laser pulses, where, e.g., the phase effects may become important, as these effects break the symmetry over the azimuthal angle and facilitate the average OAM transfer.

Discussions concerning the absorbed angular momentum in the literature usually start with defining a laser wave with a well-defined OAM, which are Laguerre-Gaussian beams. It is important, however, to take into account the corrections to the lowest orders of the paraxial and the slowly varying envelope approximations. Consider the simulations parameters, discussed in the previous section, and use the approximations for the electromagnetic field, rather than the numerical solution of the Maxwell with the algorithms provided by the PIC code. Namely, take the first orders of the paraxial and the slowly varying envelope approximations. The equations of motion were then solved numerically in a developed PYTHON code for individual particles, distributed as in previous simulations. In the first simulations, consider the electromagnetic field as

$$H_x = -E_y = E_0 g(t - z/c) \mathrm{Re}\left(e^{i\omega_0(t - z/c)} \frac{u_{\mathrm{pl}} + u_{\mathrm{qm}}}{\sqrt{2}} \right),$$

$$H_y = E_x = 0,$$

$$H_z = -E_0 g(t - z/c) \mathrm{Re}\left(i e^{i\omega_0(t - z/c)} \frac{\partial}{\partial x} \frac{u_{\mathrm{pl}} + u_{\mathrm{qm}}}{\sqrt{2}} \right),$$

$$E_z = E_0 g(t - z/c) \mathrm{Re}\left(i e^{i\omega_0(t - z/c)} \frac{\partial}{\partial y} \frac{u_{\mathrm{pl}} + u_{\mathrm{qm}}}{\sqrt{2}} \right), \quad (91)$$

which is the first two paraxial approximation orders and the main envelope approximation order for the boundary conditions (80).

The other considered simulation takes into account the corrections according to

$$
\begin{aligned}
\mathbf{H} = E_0 \mathrm{Re} &\Bigg\{ \Bigg[g(t - z/c)\big(\boldsymbol{\mathcal{H}}^{\{0,0\}} + \boldsymbol{\mathcal{H}}^{\{0,1\}} \\
&+ \boldsymbol{\mathcal{H}}^{\{0,2\}} + \boldsymbol{\mathcal{H}}^{\{0,3\}}\big) \\
&+ \frac{1}{\omega_0} g'(t - z/c)\big(\boldsymbol{\mathcal{H}}^{\{1,0\}} + \boldsymbol{\mathcal{H}}^{\{1,1\}}\big) \Bigg] e^{i\omega_0(t - z/c)} \Bigg\}, \\
\mathbf{E} = E_0 \mathrm{Re} &\Bigg\{ \Bigg[g(t - z/c)\big(\boldsymbol{\mathcal{E}}^{\{0,0\}} + \boldsymbol{\mathcal{E}}^{\{0,1\}} \\
&+ \boldsymbol{\mathcal{E}}^{\{0,2\}} + \boldsymbol{\mathcal{E}}^{\{0,3\}}\big) \\
&+ \frac{1}{\omega_0} g'(t - z/c)\big(\boldsymbol{\mathcal{E}}^{\{1,0\}} + \boldsymbol{\mathcal{E}}^{\{1,1\}}\big) \Bigg] e^{i\omega_0(t - z/c)} \Bigg\}, \quad (92)
\end{aligned}
$$

where the first three terms of the expansion in powers of λ_0/w_0 and the first two terms of expansion in powers of $(\omega_0 \tau)^{-1}$ are taken into consideration.

The obtained gained average values after numerical integration, i.e., the kinetic energy, the longitudinal, and the angular momentum of electrons, are shown in Figs. 9. One can see that the longitudinal momentum and the angular momentum are rather different from the results, obtained with use of the PIC-calculated fields, if only the few lower orders of the approximations for the wave are used. Instead, the consideration of the wave with the corrections (92) results in a much better agreement between the values obtained with the use of the PIC code. Moreover, it is quite interesting to note that the gained momentum and angular momentum considerably decrease when the corrections are taken into account. So, the use of a rough approximation for the electromagnetic fields may result in a substantial overestimation of the average gained quantities.

It is worth noting that within the approach used for the angular momentum gain (70), it appears that the first-order correction of the slowly varying envelope approximation may have the contribution of the order of $m_e c^4 a_0^4 \tau_{\mathrm{int}}^2 / w_0^2 \omega_0$, which is the same as the contribution of the previous orders. This is due to the fact that the lowest order of this approximation turns to zero after averaging over azimuthal angle φ_0. The second term in (70) is related to the longitudinal motion of the particle, as may be seen from (64). The influence of the longitudinal motion on the angular momentum transfer is discussed in [8].

It is interesting to note that the condition (9), used to obtain (27), is satisfied for the lowest orders of paraxial and slowly varying approximations of the electromagnetic fields arising from the boundary condition (50) with $g(t) = \cos^2(\frac{t - \tau/2}{\tau}\pi)$ when $|t - \tau/2| < \tau/2$, and 0 otherwise. When the envelope function is $g(t) = \frac{1}{\sqrt{2\pi}} e^{-(t - t_0)^2/2\tau^2}$, this condition for the lowest orders of paraxial and slowly varying approximations is satisfied with exponential accuracy. However, the condition (9) is not always satisfied, e.g., for unipolar plane waves, such as $\mathbf{E} = E_0 e^{-(t - z/c)^2/2\tau^2} \mathbf{e}_x$, $\mathbf{H} = E_0 e^{-(t - z/c)^2/2\tau^2} \mathbf{e}_y$. Such plane waves are not discussed in this paper.

The intensity of a Laguerre-Gaussian beam has a form of several rings with a center on the axis of the beam and radius $\sim w_0$. This allows one to assume that electrons gain angular momentum mostly in the regions of these rings and hence form a solenoid with a characteristic radius $\sim w_0$. According to the model of generation of the magnetic field by a solenoid with charged current [7], the magnetic field value may be estimated (in CGS units) as $H \sim en_0 w_0 v_\varphi / c \sim \frac{en_0 c^3 a_0^4 \tau_{int}^2}{\omega_0 w_0^2}$. For the parameters, normal for modern laser experiments, $\omega_0 = 2.3 \times 10^{15}$ s^{-1}, $w_0 = 1.3$ μm, $\tau = 12\pi/\omega_0$, $a_0 = 1$, and $n_0 = 0.01\, n_c$, where n_c is the critical plasma density, and the magnetic field may be estimated as $H \sim 60\, T$.

It may be noted that electrons mostly gain angular momentum of the opposite sign to that of the laser beam. The direction of the rotation of the electrons corresponds to the generated magnetic field directed along the laser beam propagation direction. This is an interesting result, which was also observed in full-scale 3D PIC simulations [7,8].

In this work, no collective effects were considered. Of course, the collective effects, as well as effects which dephase the particle motion in the wave, such as collisions, ionization, radiation friction, and others, may qualitatively change the interaction process, though it is easy to find the conditions when the single-particle processes dominate. What is actually done in the work is the initial step towards the understanding of the OAM transfer from light waves to single particles, in a situation where the particle distribution is isotropic so that there is no initial axial asymmetry in the system except the laser wave phase. The important result obtained here is that indeed, in this situation, the OAM may be transferred to the particles, and the process efficiency grows with the increasing of the field amplitude and the decreasing of the beam waist.

ACKNOWLEDGMENTS

APPENDIX

1. Table integrals

In the calculation of the electromagnetic fields using the boundary condition at $z = 0$, the integration over angle φ results in the Bessel function,

$$2\pi i^s J_s(z) = 2\pi i^{|s|} J_{|s|}(z) = \int_0^{2\pi} d\varphi \exp[is\varphi + iz\cos\varphi],$$
(A1)

with integer s,

$$H_\alpha(\omega, \mathbf{k}_\perp, z = 0) = 2\pi w_0^2 g_{\omega-\omega_0} E_0 \sum_{p,l} a_{pl\alpha} i^{|l|} e^{-il\theta}$$

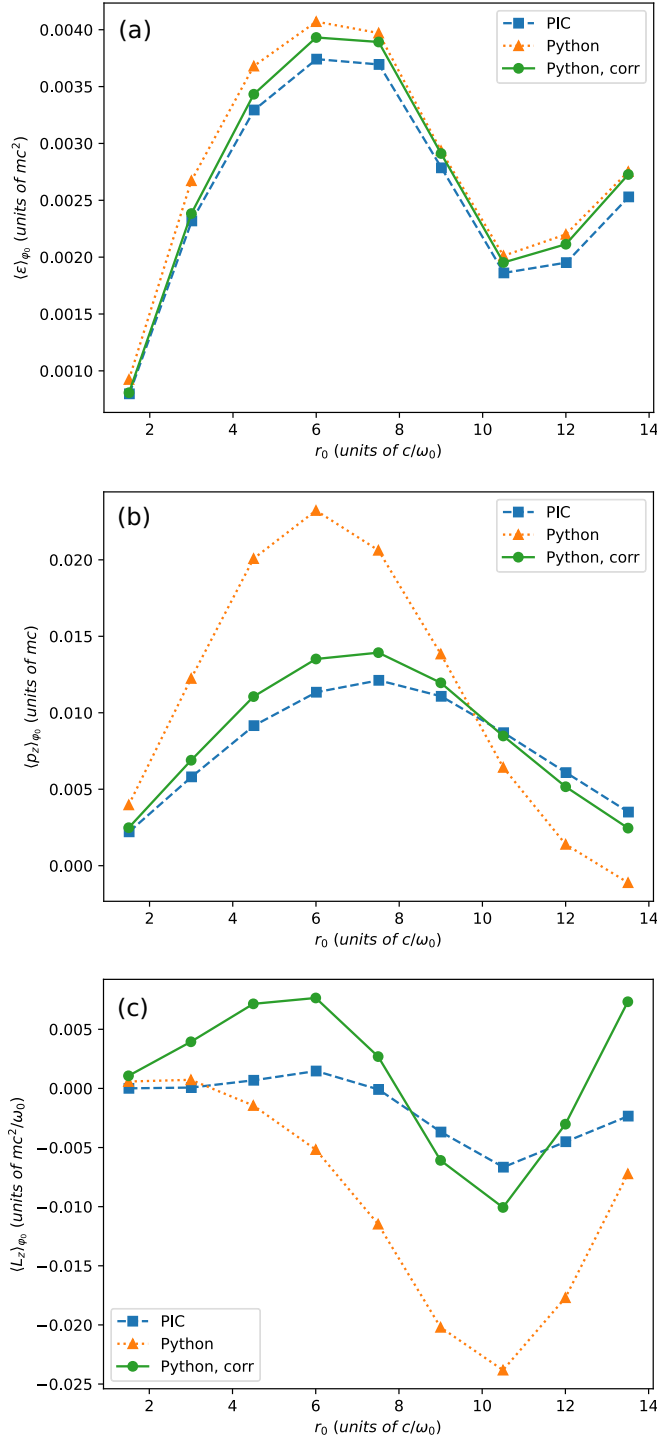$$\times \int \mathrm{r} dr U_{pl}(\mathrm{r}, 0) J_{|l|}(k_\perp r_\perp). \quad \text{(A2)}$$

FIG. 9. Average (a) kinetic energy, (b) longitudinal, and (c) angular momenta gained by electrons after the interaction with the $l = 1$, $m = 3$ beam as a function of initial distance of the particle from the beam axis. Blue squares represent PIC code numerical results; orange triangles represent PYTHON code numerical results with a few low-order approximations. Green dots represent PYTHON code numerical results with more corrections to the lowest-order approximations. For a better appearance, squares, triangles, and dots are connected with straight lines.

Using the following identity from [21] for an integral of Laguerre polynomials $L_n^s(z)$ with Bessel functions $J_s(z)$ (here, n, s, a, b are parameters):

$$\int_0^\infty x^{s+1} e^{-bx^2} L_n^s(ax^2) J_s(xy)\,dx = \frac{(b-a)^n}{2^{s+1} b^{s+n+1}} y^s e^{-\frac{y^2}{4b}} L_n^s\left(\frac{ay^2}{4b(a-b)}\right), \tag{A3}$$

after integrating (A2) over $\mathtt{r}$, one obtains (54).

2. Expressions for the fields in terms of the used approximations

$$\widetilde{\mathbf{E}}_\perp^{\{\mathbf{0},0\}} = E_0 g(\xi)\boldsymbol{\mathcal{E}}_\perp^{\{\mathbf{0},0\}} e^{i\omega_0\xi}, \quad \widetilde{\mathbf{E}}_\perp^{\{\mathbf{1},0\}} = \frac{E_0}{\omega_0} g'(\xi) iz \frac{\partial \boldsymbol{\mathcal{E}}_\perp^{\{\mathbf{0},0\}}}{\partial z} e^{i\omega_0\xi},$$

$$\widetilde{\mathbf{E}}_\perp^{\{\mathbf{0},2\}} = \frac{E_0 c}{\omega_0} g(\xi)\left[\frac{z}{2i}\frac{\partial^2 \boldsymbol{\mathcal{E}}_\perp^{\{\mathbf{0},0\}}}{\partial z^2} - i\mathbf{e}_x\left(\frac{\partial \mathcal{H}_z^{\{\mathbf{0},1\}}}{\partial y} - \frac{\partial \mathcal{H}_y^{\{\mathbf{0},0\}}}{\partial z}\right) - i\mathbf{e}_y\left(\frac{\partial \mathcal{H}_x^{\{\mathbf{0},0\}}}{\partial z} - \frac{\partial \mathcal{H}_z^{\{\mathbf{0},1\}}}{\partial x}\right)\right] e^{i\omega_0\xi}, \tag{A4}$$

$$\widetilde{H}_z^{\{\mathbf{0},1\}} = E_0 g(\xi)\mathcal{H}_z^{\{\mathbf{0},1\}} e^{i\omega_0\xi}, \quad \widetilde{E}_z^{\{\mathbf{0},1\}} = E_0 g(\xi)\mathcal{E}_z^{\{\mathbf{0},1\}} e^{i\omega_0\xi},$$

$$\widetilde{H}_z^{\{\mathbf{1},1\}} = \frac{E_0}{\omega_0} g'(\xi) i\frac{\partial}{\partial z}\left(z\mathcal{H}_z^{\{\mathbf{0},1\}}\right) e^{i\omega_0\xi}, \quad \widetilde{E}_z^{\{\mathbf{1},1\}} = \frac{E_0}{\omega_0} g'(\xi) i\frac{\partial}{\partial z}\left(z\mathcal{E}_z^{\{\mathbf{0},1\}}\right) e^{i\omega_0\xi},$$

$$\widetilde{H}_z^{\{\mathbf{0},3\}} = \frac{E_0 c}{\omega_0} g(\xi)\left(\frac{z}{2i}\frac{\partial^2 \mathcal{H}_z^{\{\mathbf{0},1\}}}{\partial z^2} - i\frac{\partial \mathcal{H}_z^{\{\mathbf{0},1\}}}{\partial z}\right) e^{i\omega_0\xi}, \quad \widetilde{E}_z^{\{\mathbf{0},3\}} = \frac{E_0 c}{\omega_0} g(\xi)\frac{z}{2i}\frac{\partial^2 \mathcal{E}_z^{\{\mathbf{0},1\}}}{\partial z^2} e^{i\omega_0\xi}, \tag{A5}$$

where $\boldsymbol{\mathcal{E}}_\perp^{\{\mathbf{0},0\}} = -\mathbf{e}_z \times \boldsymbol{\mathcal{H}}_\perp^{\{\mathbf{0},0\}}$, $\mathcal{H}_z^{\{\mathbf{0},1\}} = -i\frac{c}{\omega_0}\nabla_\perp \cdot \boldsymbol{\mathcal{H}}_\perp^{\{\mathbf{0},0\}}$, $\mathcal{E}_z^{\{\mathbf{0},1\}} = -i\frac{c}{\omega_0}(\nabla_\perp \times \boldsymbol{\mathcal{H}}_\perp^{\{\mathbf{0},0\}})_z$.

[1] L. D. Landau and E. M. Lifshitz, *The Classical Theory of Fields*, 4th ed. (Butterworth-Heinemann, Oxford, UK, 1980).

[2] V. Tikhonchuk, P. Korneev, E. Dmitriev, and R. Nuter, High Energy Density Phys. **37**, 100863 (2020).

[3] P.-V. Toma, S. Micluţa-Câmpeanu, M. Boca, and V. Băran, AIP Adv. **14**, 065109 (2024).

[4] E. Molnár and D. Stutman, Laser Part. Beams **2021**, e11 (2021).

[5] E. Dmitriev and P. A. Korneev, Bull. Lebedev Phys. Inst. **50**, S891 (2023).

[6] E. Dmitriev and P. A. Korneev, Bull. Lebedev Phys. Inst. **49**, 48 (2022).

[7] R. Nuter, P. Korneev, I. Thiele, and V. Tikhonchuk, Phys. Rev. E **98**, 033211 (2018).

[8] R. Nuter, P. Korneev, E. Dmitriev, I. Thiele, and V. T. Tikhonchuk, Phys. Rev. E **101**, 053202 (2020).

[9] Y. Shi, J. Vieira, R. M. G. M. Trines, R. Bingham, B. F. Shen, R. J. Kingham *et al.*, Phys. Rev. Lett. **121**, 145002 (2018).

[10] V. I. Berezhiani, S. M. Mahajan, and N. L. Shatashvili, Phys. Rev. E **55**, 995 (1997).

[11] S. Ali, J. R. Davies, and J. T. Mendonca, Phys. Rev. Lett. **105**, 035001 (2010).

[12] A. Longman and R. Fedosejevs, Phys. Rev. Res. **3**, 043180 (2021).

[13] I. Thiele, S. Skupin, and R. Nuter, J. Comput. Phys. **321**, 1110 (2016).

[14] P. González de Alaiza Martínez, G. Duchateau, B. Chimier, R. Nuter, I. Thiele, S. Skupin, and V. T. Tikhonchuk, Phys. Rev. A **98**, 043849 (2018).

[15] B. Quesnel and P. Mora, Phys. Rev. E **58**, 3719 (1998).

[16] L. Allen, M. W. Beijersbergen, R. J. C. Spreeuw, and J. P. Woerdman, Phys. Rev. A **45**, 8185 (1992).

[17] L. Zhang, T. Geng, X. Gao, S. Zhuang, and J. Lian, J. Opt. Soc. Am. A **35**, 1599 (2018).

[18] R. Uren, S. Beecher, C. R. Smith, and W. A. Clarkson, IEEE J. Quantum Electron. **55**, 1 (2019).

[19] A. Longman, C. Salgado, G. Zeraouli, J. I. Apiñaniz, J. Antonio Pérez-Hernández, M. K. Eltahlawy, L. Volpe, and R. Fedosejevs, Opt. Lett. **45**, 2187 (2020).

[20] J. Derouillat, A. Beck, F. Pérez, T. Vinci, M. Chiaramello, A. Grassi, M. Flé, G. Bouchard, I. Plotnikov, N. Aunai, J. Dargent, C. Riconda, and M. Grech, Comput. Phys. Commun. **222**, 351 (2018).

[21] I. S. Gradshteyn and I. M. Ryzhik, *Table of Integrals, Series and Products*, 7th ed. (Elsevier, USA, 2007).